LUND UNIVERSITY

Diffuse dust at Boliden Bergsöe investigated through X-ray Fluorescence Spectroscopy

Marcus Norlin and Linnea Savér

Master Thesis

Ergonomics and Aerosol Technology | Faculty of Engineering LTH | Lund University | 2022

Supervisor: Axel Eriksson
Assistant Supervisor: Adam Kristensson
Examiner: Christina Isaxon

Abstract

Boliden Bergsöe operates a secondary lead smelter for recycling of lead-acid batteries, located in the industrial area of Landskrona. Measurements to monitor levels of airborne particles have been conducted in several locations in Landskrona since 1977. To increase the knowledge of diffuse dust emission sources at Boliden Bergsöe, airborne metal concentrations were measured in ambient air for eight consecutive days using on-line X-ray fluorescence spectroscopy. Sampling was done with time resolutions of one and two hours during the period 5th - 13th of March. It was first suspected that handling of slag in the area called Slaggplan, was the main origin of diffuse dust. Activities related to slag handling were therefore logged using surveillance footage and compared with measured concentrations to investigate whether this suspicion was justified. The measurements showed that lead (Pb) was the largest constituent of the elements measured at an average of 1464 ng/m^3. Furthermore, Pb concentrations followed a diurnal trend with large peaks during daytime. Peaks usually coincided with an increase in temperature and decrease in relative humidity, indicating that dust accumulated on the ground during the night and resuspended during the day, after the ground had dried. There was no clear relationship between the Pb concentrations and the slag handling activities, implying that slag handling was not likely the main origin of the airborne Pb. Instead, it was concluded that lead paste and filter dust were more likely origins of diffuse dust, since their element compositions better reflected the measured concentrations at Boliden.

Populärvetenskaplig sammanfattning

I detta arbete försöker vi reda ut vad det är som orsakar diffus damning på en industrianläggning i Landskrona, drivet av ett företag som heter Boliden Bergsöe. De spelar en viktig roll för miljön eftersom de återvinner bly-syra-batterier som finns i bilar och andra elektriska fordon. Tyvärr innebär hanteringen av bly att en del utsläpp av detta grundämne sker till den kringliggande miljön. Bly har förmågan att uppehålla sig länge i marken och om ett område är kontaminerat med bly kan upptaget av ämnet hos människor, djur och växter öka. För att kunna minska spridningen av bly, måste man först ta reda på varför det uppstår blydamm på Boliden. Detta är examensarbetets främsta mål.

Bara genom att titta i riktning åt Boliden redan från Landskrona station, finner man en misstänkt källa; skorstenen som transporterar processgaser från produktionen till en utsläppskälla långt över marken. Däremot har Boliden, precis som andra tyngre industrier i Sverige, ett system för att rena processgaser. Dessutom är själva syftet med att ha en skorsten är att emissioner sprids och späds ut över större områden, helst utanför den egna staden. Ett mer troligt ursprung till blydammet i närområdet är så kallade diffusa dammkällor som kommer från Boliden på marknivå. Exempel på diffusa dammkällor är materialhögar med finkorniga material. När dessa befinner sig utomhus kan de börja damma om det börjar blåsa, om fordon hämtar material från dem eller om de störs på annat vis. Damm kan också samlas på marken under en tid och sedan lämna marken på grund av att trafik, vind eller andra fysiska krafter påverkar dammet.

Våra mätningar visade att blyhalten i luften är betydligt högre på dagen än på natten. Denna observation ledde oss till slutsatsen att blydamm hamnar i luften till följd av resuspension. Resuspension innebär att ett dammigt material först hamnar på marken för att sedan hamna i luften vid ett senare tillfälle. Just på natten var marken fuktig, vilket förklarar varför partiklar inte har kunnat lämna marken på natten. När det sedan blivit torrt har antingen trafik, vind eller andra fysiska krafter orsakat att dammet lämnat marken.

Hur ska man då förhindra att dammet lämnar marken? Det finns olika sätt att minska resuspension, bland annat genom att inte låta utomhusytor torka upp. Detta kan däremot svara svårt om solen skiner under stora delar av dagen och om det är stora områden som skulle behöva vätas för att hålla marken fuktig. En annan strategi inriktad på prevention av dammutsläpp kan snarare vara i ordning; att förhindra att dammet hamnar utomhus överhuvudtaget. Genom dialog med företaget fick vi nämligen veta att blypasta, vilket är en av mellanprodukterna i processen, har en tendens att samlas innanför portar och att blypastan kan fastna på fordon som kör med våta däck. Vårt främsta förslag till företaget blev alltså att försöka hindra denna blypasta från att ta sig ut, kanske genom att begränsa trafiken som kör in och ut från processanläggningen.

Acknowledgements

We would like to thank our thesis supervisor Axel Eriksson and assistant supervisor Adam Kristensson for your commitment and valuable insights, as well as help and support during this project.

We would also like to thank Mårten Strömberg, Hanna Lejon and other employees at Boliden Bergsöe for your help, interesting discussions and for providing useful data and insights, improving the quality of the project.

Table of Contents

1. Introduction & Purpose

Boliden Bergsöe (hereafter referred to as Boliden and not to be mistaken for the Swedish municipality of the same name) is a company in Landskrona which operates a lead smelter for recycling of spent lead-acid batteries. This process is also referred to as secondary lead smelting. Since the recycling process at Boliden involves handling of lead, they are under scrutiny by local governments in accordance with the environmental laws of Sweden. As a result, the company is incentivized to manage their emissions to the environment.

For the last decades, the general exposure to lead has decreased in Sweden, which can largely be attributed to the prohibition of leaded petrol. Even in Landskrona, where Boliden operates its lead smelter, the lead-levels in blood of children have decreased to levels close to the average levels of children in the rest of the country. There have also been aerosol measurements in Landskrona for measuring the amount of metals in the ambient air, where lead concentrations have been within threshold values.

Although lead concentrations in ambient air and in the blood of children have not given reason for concern in Landskrona, lead may still introduce an environmental and health problem if it is distributed on ground surfaces and in the water of the surrounding area. Local governments are therefore still calling upon the company to maintain its responsibility in understanding and mitigating their emissions, particularly of lead, to the environment. This thesis work concerns one type of such emissions, known as diffuse dust emissions

The Swedish Environmental Institute explains that the definition of diffuse dust "includes dust from diffuse sources such as bare surfaces, material deposits, stone crushers and resuspension of dust by work machines" (Gustafsson, Saucedo, Rosendahl, & Lindén, 2020). They explain that diffuse dust emissions differ from point source emissions, e.g. from a chimney, in that the prior are more difficult to define, quantify and manage. However, "diffuse sources" are included in the formal definition of emissions in the EU Directive concerning integrated pollution prevention and control (1996/61/EC). This means diffuse dust is implemented in regulation, although difficulties in quantifying and managing the problem remain.

The purpose of this work was to increase the knowledge about diffuse dust sources at the Boliden facility, in order to help the company make informed decisions when implementing mitigation strategies for managing these emissions. To measure the diffuse dust emissions at Boliden, an Xact 625i Multi Metals Monitor (further referred to as Xact) was used. This allowed for measuring concentrations of certain elements in the PM_{10}-fraction at a time resolution of 60-120 minutes. The report aims to answer the following research questions:

- What is/are the origin material/s of the diffuse dust emissions and by what mechanisms are they released into the ambient air?
- Is the application of on-line X-ray Fluorescence technology suitable for investigating diffuse dust emissions in industrial settings?

Note that quantification of diffuse dust generation from sources at Boliden is not included in the purpose. As will be described in 2.2, other methods are conventionally used for quantification of diffuse dust.

2. Background and theory

2.1. Atmospheric aerosols

Aerosols are solid or liquid particles between a couple of nm to 100µm suspended in the atmosphere. Particles can be formed by primary sources or secondary sources. Examples of primary sources are mechanical generation, such as mechanical grinding; windblown dust and wave breaking; combustion processes such as biomass combustion and engine combustion; or as biological particles such as pollen and bacteria. Secondary particle sources are particles formed from gaseous precursors.

Particulate matter can be divided into coarse particles, and fine particles. Particulate matter with an aerodynamic diameter smaller than 10 and 2.5 µm are referred to as PM_{10} and $PM_{2.5}$ respectively. The size of a particle can, for example affect how deep into the respiratory system it can be deposited and the mechanism of deosition. Its size is therefore an important factor for health effects associated with aerosols (World Health Organization, 2021). The ability of a particle to remain airborne, rather than settle on a surface, also depends on its size. Larger particles have a higher terminal settling velocity and are therefore more prone to settling due to gravity than smaller particles.

Particles below 1 µm typically remains airborne for about a week and can be transported thousands of kilometers, with the exception of particles below 100 nm that can settle by diffusion. Particles in the coarse fraction can remain airborne for several days and be transported several hundreds of kilometers from the source (World Health Organization, 2006). A transition between long-term (days and weeks) and short-term (minutes and hours) suspension occurs around 20 µm particle size. Particles suspended short-term can travel between a couple of meters up to roughly one kilometer. The limit for short-term suspension is around 70 µm (Nickling & Neuman, 2009) although particles up to 100 µm can become airborne.

Particles can deposit on surfaces through both dry and wet deposition, the latter meaning scavenging by rain or snow (Nicholson K. W., 2009). Conditions may allow for particles to resuspend from the surface after deposition and become airborne again. Resuspension occurs when aerodynamical or mechanical forces exceed the adhesion forces between the particles and the surface they reside on. Models that predict resuspension rates have been developed and compared to experimental data under different conditions (see e.g. (Stempniewicz, Zhipeng, Yanhua, & Komen, 2018)). Wind-tunnel experiments have shown that resuspension rate, which is the fraction of deposited material removed per unit time from a surface, increases drastically at high wind speeds for larger particles on concrete and grass surfaces. The effect of wind speed is not as distinct for smaller particles, including PM_{10}. Results from these experiments on concrete are shown in Figure 1. From the same experiments, it was found that resuspension rate decreases sharply with time after deposition of material, meaning most particles resuspend early (within thirty minutes) after conditions allow this. Moisture in material tends to increase surface adhesion forces of deposited material and practically eliminate the tendency for resuspension (Nicholson K. W., 2009).

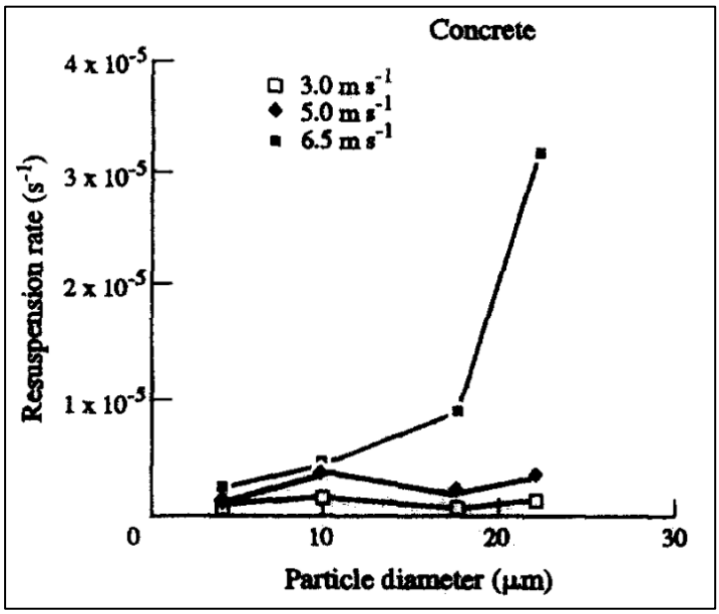

Figure 1: The dependence of resuspension rate on particle diameter and wind speed from wind tunnel experiments conducted by Nicholson (1993).

Saltation is one of the main mechanisms by which resuspension of small particles is induced on sand dunes. It means large particles (>100 µm) "hop" across the surface (saltate) at sufficient wind speeds and, upon impaction, cause smaller particles to leave the ground (Kok, Parteli, Michaels, & Karam, 2012). In urban environments, vehicles are commonly considered the most significant cause of resuspension of road dust (Nicholson, 2009).

Aerosol particles present in the air can be measured using different techniques. For instance, Sina et al. (2020) used the Xact 625i Multi Metals Monitor to monitor the air in the Los Angeles area. By using the Xact, the authors found diurnal, daily and seasonal trends in element concentrations and could identify sources for the measured elements using positive matrix factorization. The study used wind data in combination with the concentration measurements to find the most probable locations of the sources. Due to the high temporal resolution, Sina et al. (2020) were able to measure the daily variation in Fe concentration, which was higher during daytime than night time. The authors attributed the cyclic nature of airborne Fe to soil resuspension occurring during daytime as a result of higher wind speeds and temperature, as well as lower air humidity. Another study which took advantage of hourly sampling times was conducted by Berger, Berger & Skerratt (2019), who also coupled data on wind direction to assess the contribution to airborne lead from ships that were loading lead and zinc in a port.

2.2. Diffuse dust

In this section, information from previous work relating to both diffuse dust in industrial settings and dust in urban environments is presented. After surveying literature on diffuse dust, it became apparent that the term "diffuse dust" is mainly an industrial term. However, other sources were found who were not necessarily concerned with the dust being of "diffuse" origins, yet still provided useful information for developing a holistic view of dust phenomena. This information would also prove relevant for drawing conclusions regarding the diffuse dust emissions at Boliden.

Mechanical breakdown of materials can generate primary airborne dust through processes such as grinding or crushing of materials (World Health Organization, 1999). Diffuse dust is defined as dust which is not released from a point source. An example of a point source would be a chimney or other exhaust system. Dust generated by dispersal of powder when transferring, dumping, or filling of granular material are examples of diffuse dust sources. Passive dust emissions from deposits of granular material can also be considered diffuse sources.

Dust emissions from sources such as those presented above can be quantified by calculating so called emission factors. An emission factor is defined as the amount of dust generated from an activity per unit time, distance traveled or some other category. US EPA (1986) provides a standard for calculating emission factors. The total emissions from an activity must first be measured before an emission factor can be calculated. One method of measuring emissions from diffuse dust sources is by using dust monitors with high-frequency measurements (seconds) to establish the amount of dust originating from a certain activity (see e.g. Martín et al. (2007) and Gustafsson & Petersson (2016)). As mentioned earlier, the purpose of this work was not to quantify diffuse dust generation from activities at Boliden. However, an attempt was made at investigating if there was a direct relationship between certain activities at Boliden and elevated concentrations of aerosols, further described in 3.4.

Although diffuse dust may be generated by an industrial activity, dust may not leave the confines of the industry immediately. It could also deposit on the ground and surfaces in the ambient environment, only to be disturbed by traffic for example, as seen in Figure 2. In this case, dust is generated by a diffuse dust source but the mechanism of it spreading to the environment would be resuspension. This phenomenon was described previously in 2.1.

Surface characteristics of trafficked areas have been shown to significantly affect the amount of dust suspended in the air. Dust emissions from traffic on gravel roads are higher compared to concrete roads, which is one of the reasons for asphalted surfaces being recommended in trafficked areas (Gustafsson, Saucedo, Rosendahl, & Lindén, 2020). Seasonal variability can also affect the tendency for resuspension. A study on four of the busiest streets in Stockholm, Sweden, showed that accumulation of dust was favored over resuspension while surfaces retained high moisture levels, in accordance with the theory presented by Nicholson (2009). Furthermore, Gustafsson, Blomqvist, Johansson, & Norman (2012) found PM_{10}-concentrations to be particularly high once surfaces dried up after road dust had accumulated over a period of time. Measurements that are conducted over a shorter period of time as in this thesis work (days) can therefore not be said to represent the dust tendencies throughout a month or a year.

Figure 2: Example of dust resuspension as a dumper is driving over a concrete surface. Note that the surface is covered to a large degree in granular materials. Pictures taken from Gustafsson, Saucedo, Rosendahl & Lindén (2020).

Dust can also be blown from deserts such as Sahara and contribute to PM_{10} in Europe by long range transport (Mallone, et al., 2011). When dust storms occur, dust in the coarse particle

fraction can be transported more than 1000 km from its source (World Health Organization, 2006). No such dust storms were known to occur at the time of the measurement campaign of this thesis work.

2.3. Health effects

The health effects of dust exposure are dependent on the type of dust, as well as the size distribution of the dust, its concentration, and the exposure time of an individual. For example, accumulation of dust in the lung can lead to pneumoconiosis and potentially causing changes in lung function such as byssinosis, caused by cotton dust, or silicosis, caused by crystalline silica dust. (World Health Organization, 1999). However, the focus of the report is the origin and mechanisms of the diffuse dust and not the health effects.

Where in the respiratory system that aerosols deposit depends on several factors, such as particle size, geometry of the airways and the shape of the particle. The respiratory system can be divided into three main parts, the head airways, the tracheobronchial region, and the alveolar region. The main mechanisms by which aerosols deposit are impaction, settling and diffusion. Deposition by impaction mostly occurs for larger particles with a higher inertia in the large airways. Ultrafine particles, particles with a diameter less than 100 nm, can also deposit in the head airways by diffusion. In the smaller airways and alveolar region settling and diffusion are favored by the low flow velocities and smaller dimensions (Hinds, 1999). The deposition probability of particles in different regions of the respiratory system is shown in Figure 3.

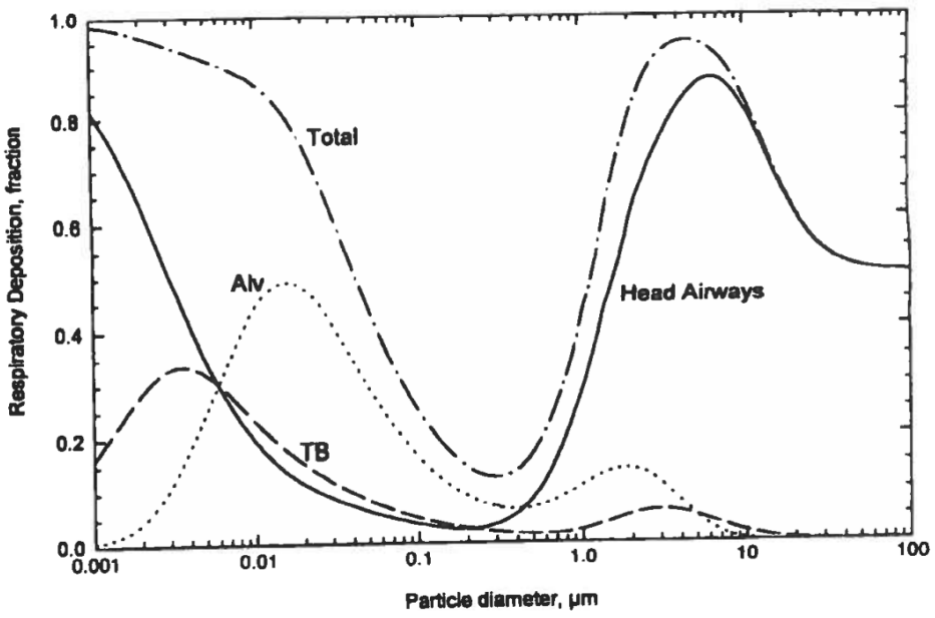

Figure 3: Deposition fraction in the respiratory system as a function of particle diameter (Hinds, 1999)

2.4. Lead dust

The general exposure to lead can have several different sources, such as lead-based paint, leaded fuel and industrial emissions from battery manufacturing or recycling, lead smelting and mining (Wani, Ara, & Usmani, 2015). Exposure can occur through inhalation of airborne lead as well as exposure through ingestion from contaminated soils, most common in children with hand-to-mouth behavior (World Health Organization, 2007). Leaded fuel has been banned in Sweden

since 1994 and bans were introduced in most European countries in the late 90s which reduced the general concentration of airborne lead (World Health Organization, 2007). Airborne lead is a minor source of lead in most places but in close proximity to industrial sources, lead levels in the air can be significantly higher than normal background concentrations (World Health Organization, 2007). Air quality guideline values for particulate matter and airborne lead are presented in Table 1, where the inhalable fraction is the fraction of particles that can be inhaled through the nose or mouth and the respirable fraction is particles that can enter the gas-exchange region of the lungs. There is also potential for soil contamination due to lead dust escaping the confines of lead-handling facilities. One of the problems with lead is its persistence once it is emitted to the environment. Xing et al (2020) analyzed ground samples near both a closed and an active lead smelter and found that both sites had elevated lead concentrations. The study found that deposition on both sites were mainly from resuspended contaminated soil, rather than from the active lead smelter, indicating the problem of lead being persistent (Xing, et al., 2020).

A biomarker commonly used when discussing lead exposure and health effects is the lead-level in blood (B-Pb), expressed in units of μg/L or μg/dL. Lead is stored in the blood, soft tissues and the bone (World Health Organization, 2007). The biological half-life of lead is approximately a month in blood and soft tissues and decades in the bone. Blood lead levels can provide both information about recent and previous exposure (World Health Organization, 2007) (World Health Organization, 2000). Exposure to lead can affect the body in several ways. The kidneys, nervous system and blood pressure may be affected by long-term lead exposure at moderate exposure concentrations (World Health Organization, 2000). Lead dust can lead to systemic poisoning when dust in the inhalable fraction enters the respiratory system and passes to the bloodstream (World Health Organization, 1999). Children are more sensitive to lead than adults and reduced cognitive capacity may occur during long-term exposure (Rubin & Strayer, 2008). Blood lead levels of 100-150 μg/l have in epidemiological studies shown to have harmful effects on children (World Health Organization, 2007). No minimum threshold for harmful levels of B-Pb has been established (Wani, Ara, & Usmani, 2015).

Table 1: Air quality guideline values.

	Value	Type	Reference
PM_{10}	15 µg/m^3	Annual mean	(World Health Organization, 2021)
$PM_{2.5}$	5 µg/m^3	Annual mean	(World Health Organization, 2021)
Lead	0.5 µg/m^3	Yearly average	Directive 2008/50/EC (2008)
Lead	1 µg/m^3	Yearly average in immediate vicinity of specific, notified industrial source	Directive 2008/50/EC (2008)
Occupational limit value of lead, inhalable fraction	100 µg/m^3	Eight-hour exposure	AFS 2018:1
Occupational limit value of lead, respirable fraction	50 µg/m^3	Eight-hour exposure	AFS 2018:1

2.5. Landskrona industrial area

Boliden is situated in an industrial area in Landskrona city. Primarily two sources of metal dust have previously been identified in the area; Boliden Bergsöe and Befesa ScanDust. Befesa ScanDust recycle dust from filters used in the production of stainless steel (Befesa ScanDust, u.d.) and are located around 500 meters southwest of Boliden, see Figure 4. Studies have shown that metals emitted to the environment by ScanDust are mainly Cu and Zn while Boliden is the origin source of practically all lead in the fine ($PM_{2.5}$) and coarse (PM_{10}) fractions in Lundåkrahamnen (Kristensson, et al., 2019). Aside from Boliden and ScanDust, there are several smaller industries operating in the area.

Figure 4: Location of Boliden Bergsöe and Befesa ScanDust in Landskrona industrial area.

2.6. Boliden Bergsöe description

2.6.1. Lead processing

At Boliden, the recycling process starts with batteries arriving by truck, either on pallets or in other containers. They are drained from sulphuric acid when their drop of roughly five meters into a storage facility causes them to break on the floor. Batteries are then fed to the battery breaking unit where plastic is separated from the lead paste. Subsequently, the lead paste is fed into a furnace, where lead is reduced from mainly $PbSO_4$ and PbO into elemental lead. Finally, the pure lead is refined and cast into ingots. Process gases go through an afterburner and is treated with lime, before finally being cleaned through bag filters.

An overview of a typical secondary lead smelting process can be seen in Figure 5. As shown in this figure, every main process can give rise to lead emissions to the environment if they are not controlled. The method of controlling process dust emissions at Boliden is by performing all of the above operations in enclosed or semi enclosed spaces. All process buildings are connected to a ventilation system which joins the process gas system for further treatment. Any dust emissions occurring in the closed system should ideally be captured by their bag filter units. Bag filters, when designed and operated properly, are able to capture dust particles as small as 0.05 µm (depending on the technology used) at an efficiency beyond 99% (Sparks & Chase, 2013).

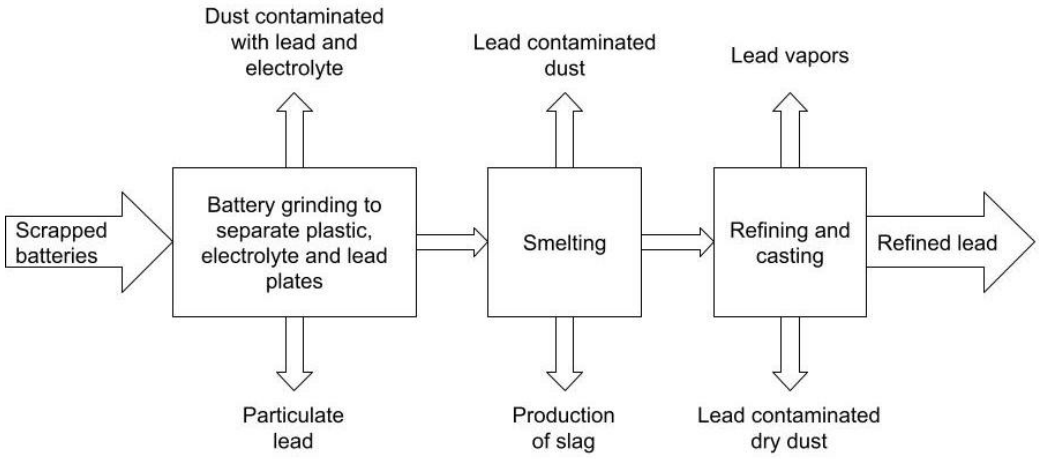

Figure 5: Block diagram of a typical secondary lead refining process as described by (Genaidy, Sequeira, Tolaymat, Kohler, & Rinder, 2009). The transport step between battery grinding and smelting in the source material has been omitted. Furthermore, only potential emissions of lead-containing particles into air have been included. Additional types of emissions unrelated to Pb are included in the source material.

Inside the processing facility, there are considerable amounts of lead paste with 10% moisture content as deposits on the ground (Strömberg M. , 2022). These have been deemed potential origins for the diffuse dust emissions by management at Boliden, as some of the lead paste attaches to the wheels of vehicles before they leave the processing facility. Such paste was preciously sampled by Boliden and its average composition is presented in Table 2.

Table 2: Composition of lead paste.

Element	Composition (%)
Pb	74.0
O	17.2
S	5.5
Si	1.8
Na	0.6
Other	0.9

The "Other" category in Table 2 includes the elements Al, Ba, Ca, Cr, Cu, Fe, Hg, K, Mg, Mn, Na, Nd, Ni, P, Sb, Sn and Zn. Particularly, Sb has been associated with the production at Boliden, as is described in Section 2.8.

Another material which has been analyzed at Boliden is filter dust from the bag filter units. Its composition is presented in Table 3. During normal operation, filter dust is collected in big bags in closed systems, preventing emissions to the environment. However, once every week, maintenance is conducted in a part of the process gas system. The purpose of the maintenance is to remove dust build-up in the gas channels. On these occasions, some dust may be handled openly in the environment, since the dust is transported in open bins from the filter units to the processing facility (see Section 0). Together, the lead paste and filter dust are the materials of the highest Pb-content which could generate diffuse emissions due to their granular structure. Both of them also contain Sb.

Table 3: Composition of filter dust.

Element	Composition (%)	Element	Composition (%)
Pb	74.0	Sb	0.47
S	8.5	Zn	0.46
Ca	4.4	Fe	0.40
Cl	1.9	Ti	0.13
Sn	1,4	Cu	0.11
Br	1,4	Cd	0.08

Slag is continually removed from the lead melt during the smelting step and is collected in pots inside the processing facility. Aside from slag, a byproduct known as matte is also extracted, as well as a small amount of elemental Pb. Due to density difference of slag, matte and Pb, they will amass in different sections of the pots, while the extracted materials are still liquid. The majority of the slag consists of Fe and Si, while the matte consists of Fe and S. Compared to the granular lead paste and filter dust, the Pb in the slag pots forms a hard shell.

After the top layer of the extract has turned solid due to cooling, the pots containing the extract are transported outside for further cooling. In the next section, activities on the outside of the facility are described, including handling of the extract. Although slag only makes up a fraction of the extract, bulk handling of the extract will further be referred to as "slag handling".

2.6.2. Overview

A satellite view of the Boliden area can be seen in Figure 6. At the time the picture was taken, a couple of material deposits existed immediately outside Boliden on the west side, visible as yellow, gray and brown mounds. It is unknown whether such deposits were present during the aerosol measurements of this report. Transport of smaller particles from these heaps could possibly occur over the perimeters of Boliden, contributing to the aerosol concentrations, depending on their tendencies for emitting dust. On the other hand, the entire perimeter of the Boliden compound is surrounded by solid planks or walls, as well as shrubby vegetation on the W side, presumably lowering the contribution from outside sources to aerosol concentrations. Practically all outside surfaces within Boliden consist of asphalted ground that are cleaned every weekday. Wet cleaning is applied on most of the surface area at Boliden when there is no risk of freezing. This means cleaning is done by spraying high-pressure water underneath a large vehicle and capturing the spray particles using a vacuum.

Figure 6: View of the entire area occupied by Boliden (within yellow border). The picture was taken in 2018.

For a more detailed view of the Boliden area and its facilities, see Figure 7 and 8. Figure 7 shows the NW part of Boliden. There is no processing of materials in this area other than transport and storage. Vehicles travel here for transporting finished goods, byproducts, or other materials. Vehicles are also washed here after they have been operating for a while.

The SW part, shown in Figure 8, houses the production facility. Just outside the production facility, on its W side, is the Slaggplan area, which will be described in closer detail in the next section. Within the blue and red borders are material deposits necessary for the recycling process. Items within the black polygons are spent batteries, waiting to be recycled. Rampen in the figure leads to another storage facility. The area between Rampen and Vågen areas are the most trafficked areas during the daytime (from ~7:00 to ~15:00). Traffic in this area is negligible on weekends.

Figure 7: View of the NW part of the Boliden Bergsöe area. Picture was taken in 2018.

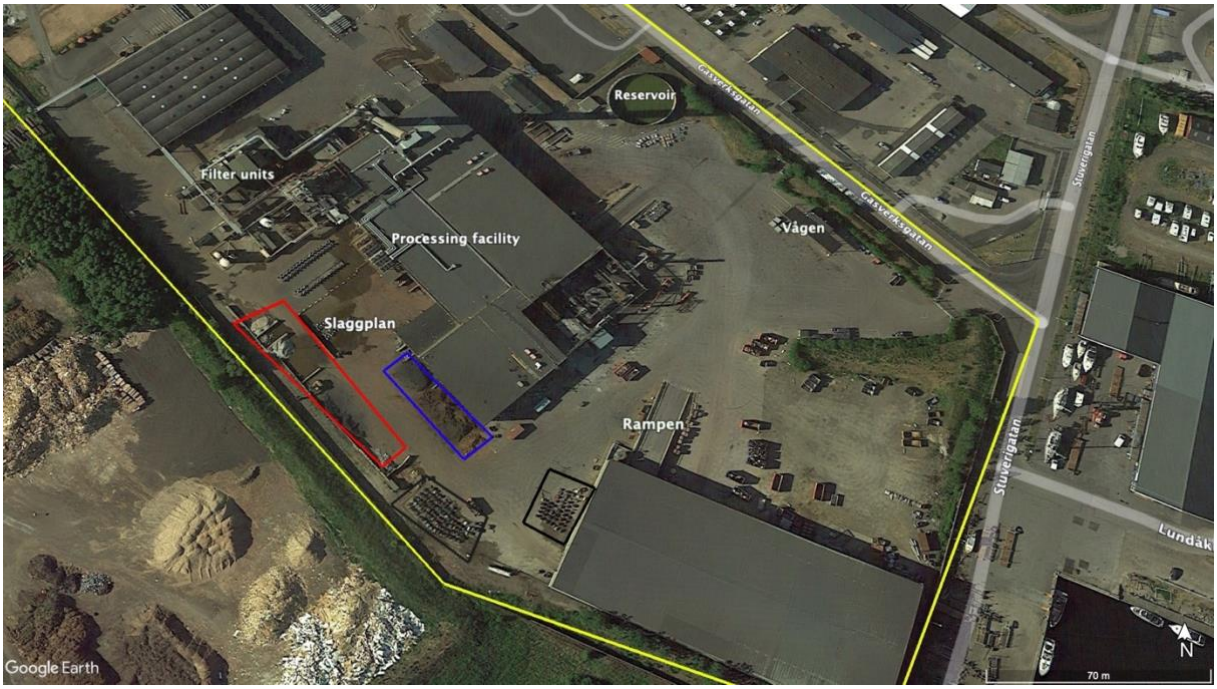

Figure 8: View of the SW part of the Boliden area. Picture was taken in 2018.

2.6.3. Slaggplan

Slaggplan is the location where slag blocks are separated into slag, for further recycling, and byproducts. A schematic of Slaggplan and activities there are shown in Figure 9. After the top layer of the slag has solidified, the slag pots are left to cool outside for further solidification. Once the contents of the slag pots are solid, they are turned upside down within the light gray square in Figure 9. This means the heavy Pb fraction will be at the top of the block. After around 10-15 slag blocks have accumulated on the light gray square, a crane is used to separate the slag fraction from the matte and Pb fractions from each block. Finally, a wheel loader transports

the slag back into the processing facility and the rest to a containment unit in the NW part of Boliden.

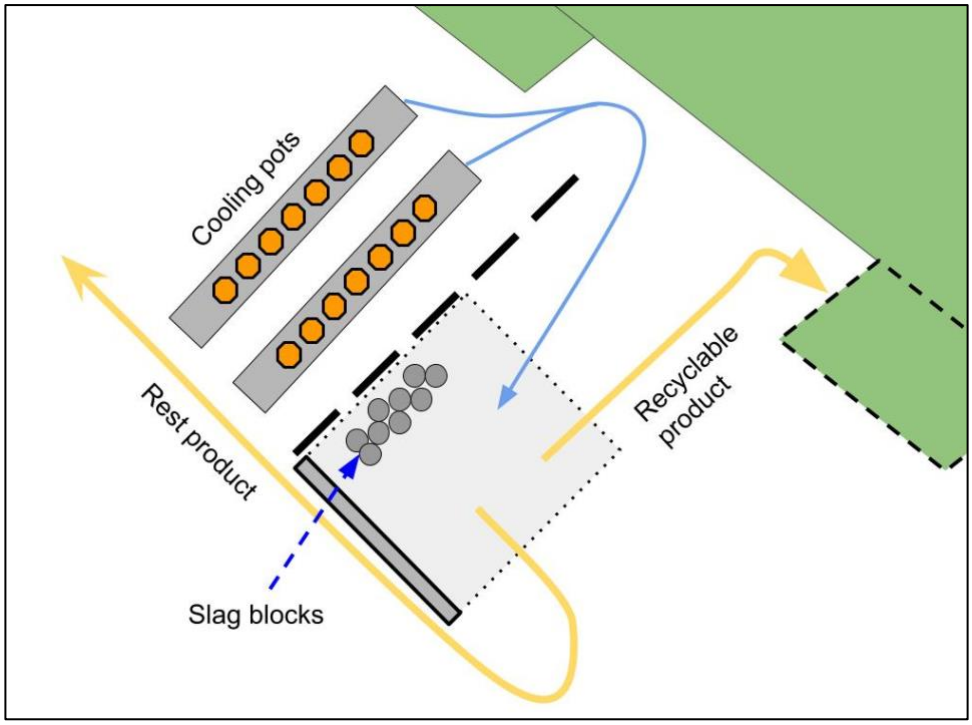

Figure 9: Schematic of Slaggplan. After cooling, pots of solid slag are emptied onto the light grey area by a small electric truck. Afterwards, slag blocks are moved by crane to another position in the light grey area. Finally, a front loader lifts the slag and recycles it to the process.

Figure 10 shows a close overview of Slaggplan. Water cannons are mounted along the wall behind the slag blocks, indicated by the light red line. These cannons shoot water towards the blocks for further cooling. As a result, the ground is often wetted in this area. On the other side of the wall, by the light blue marker, there is a sink in elevation where water can collect and form a basin. A picture of this basin is visible in Figure 11. Since heavy vehicles often travel over this basin, they spread some of the water to the surrounding ground with each pass.

Figure 10: Overview of the Slaggplan area. Along the red line are water cannons, spraying water towards the slag blocks. The blue marker shows the area of lower elevation.

Figure 11: Water basin next to the area where slag pots are emptied. This picture was taken after the measurement campaign. During the campaign, the basin was much larger and had a distinct red colour.

2.6.4. Material Deposits

Next to Slaggplan in the SE direction is a corridor for open storage of production materials. This corridor is shown in Figure 12. Materials that are stored here are iron scrap, lead scrap and coke. Wheel loaders regularly pick up and transport materials to the production facility via Slaggplan. The larger stockpiles containing iron scrap and coke are filled by trailer dumping a couple of times a week.

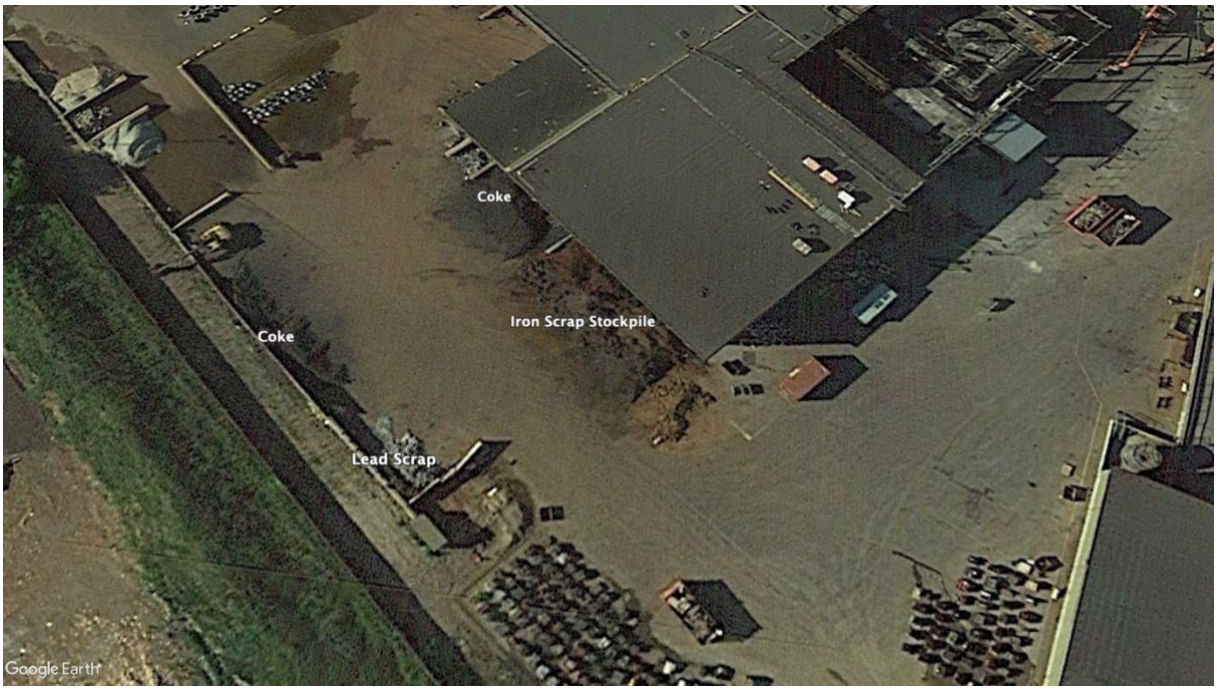

Figure 12: Overview of the stockpile corridor.

2.7. Previous measurements in Landskrona

Aerosol measurements in the Landskrona area have been conducted over several measurement periods since 1977 using two techniques; falling dust sampling and aerosol sampling (Prosper, 2017). The prior has been conducted continuously since 1988 by Landskrona city environmental management and the latter having been conducted at separate time intervals with several years between campaigns. The first studies on aerosol levels in 1977 showed higher amounts of lead than subsequent studies in 1988 and onwards. This is mostly attributed to a decrease in lead-content in petrol (Livsmedelsverket, 2022).

Separate from air measurements, blood samples from children living in Landskrona have also been examined for lead. Strömberg et al. (2008) concluded that blood lead among children from 1978 to later periods in the 2000s showed a dramatic decrease as shown in Figure 13, which coincided with the ban on lead in gasoline. Nevertheless, lead is still a concern where populations are chronically exposed to the element. Stroh et al (2009) also looked at B-Pb levels in Landskrona and discussed whether accumulation of lead in soil around the lead smelter could have contributed to the near-smelter elevation in B-Pb observed in their study.

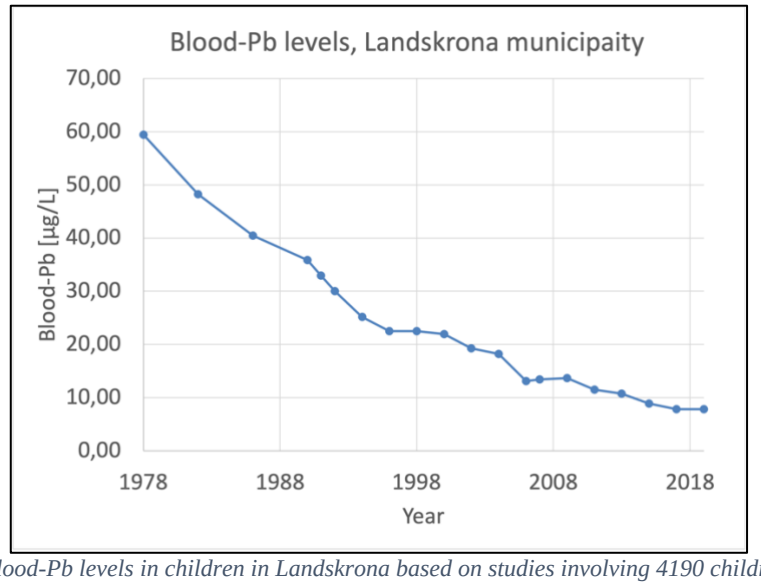

Figure 13: Average blood-Pb levels in children in Landskrona based on studies involving 4190 children between the years 1978 and 2019. Reproduced from (Landskrona stad, 2021).

Fargo et al. (1999) studied soil samples in Landskrona at different distances from the lead smelter. The soil samples were from 5 different zones, where zone 1 was the closest to the lead smelter with samples from the industrial area, and zone 5 was the furthest with a distance greater than 3.5 km from the lead smelter. The study found that all zones had higher concentrations of lead in the topsoil than the average background concentration in Sweden, with concentrations decreasing the further away from the lead smelter they were. The mean topsoil concentrations of lead in zones 1, 2 and 5 were 792, 158 and 39 µg/g respectively, compared to 14.6 µg/g which was the median lead topsoil concentration in Sweden in 1977 (Farago, Thornton, White, Tell, & Mårtensson, 1999).

The most recent aerosol measurement in Landskrona, before this campaign at Boliden, was conducted in 2017 using Particle Induced X-ray Emission (PIXE) technology (Kristensson, et al., 2019). Fine ($PM_{2.2}$) and coarse fraction (PM_{10}-$PM_{2.2}$) particulate matter was measured at two different locations; one urban environmental location, “Stadshuset”, and one industrial

location “Lundåkrahamnen”, the latter being visible in the bottom-right corner of Figure 6 (Kristensson, et al., 2019). The average concentrations of Pb and the five most abundant metals are presented in Table 4.

Table 4: Average concentration of lead measured in Stadshuset and Lundåkrahamnen in Landskrona in ng/m^3 (Kristensson, et al., 2019).

Element	Fine fraction Stadshuset	Coarse fraction Stadshuset	Fine fraction Lundåkrahamnen	Coarse fraction Lundåkrahamnen
Pb	3.9	4.4	14	21
Si	80	221	94	230
Fe	51	127	60	127
S	360	140	333	270
Cl	720	1690	421	1660
K	67	58	68	68

Kristensson et al. (2019) used a source-receptor model called positive matrix factorization (PMF) to establish the origins of the different metals measured. Their model found that Pb measured in both locations and fractions were from one Pb source, corresponding to Boliden, since high concentrations of Pb were observed when the measurement points were downwind from the facility. The concentrations of airborne Pb in the coarse fraction at the different locations were all below the average threshold value of 0.5 µg/m^3 as dictated by the EU Directive 2008/50/EC for urban environments and 1.0 µg/m^3 for industrial environments. For all other elements than Pb, Boliden only contributed little to none to their measured concentrations. A minor amount of Si, Fe and K were attributed to the Pb source, although they originated mainly from an earth dust source as well as from other industries than Boliden. Also included in the earth dust source were elements like Ca and Ni.

2.8. Previous measurements at Boliden

In 2015, there was an attempt at quantifying emission factors at Boliden using so called flux meters for passive collection of airborne particles. Flux meters consists of several collectors on a common stem, each collector pointing in different directions. Collectors are formed as tubes with their openings pointing horizontally towards the environment. The purpose of flux meters is to catch wind-driven particles and determine the directions for potential sources based on wind-data.

The resulting emission factors of this campaign were defined as the total particulate emissions for the entire Boliden site. One collector placed at Rampen, pointing in the SE direction collected 50 times higher Pb mass than the collector with the second highest Pb mass collection, leading the analysts to believe there would be a source outside of Boliden in the SE direction contributing greatly to Pb in particulate matter. This went against any previous results in the Landskrona measurements as described in the previous section. Many details about the methods of these flux meter measurements are not available, making it difficult to verify if their method provided reliable results. One important detail not available in the documentation of this campaign is the height at which flux meters were placed. For example, placing flux meters closer to the ground will entail the possibility of also collecting saltating particles (Poortinga , o.a., 2013), which might have been the reason the Rampen collected such a high mass of Pb. Conclusively, this study did not provide reliable insight into the origins of dust or the mechanisms by which it became airborne at Boliden.

Since April of 2019, Boliden has conducted falling dust measurements (further referred to as FDMs) at several locations both inside and outside of its industrial site. These measurements are also passive but have openings pointing upwards, hence collecting settling (falling) particles. Particles are collected in NILU SF1 particle fallout collectors, seen in Figure 14, through both wet and dry deposition. Samples undergo elementary analysis, determining concentrations of up to 18 elements. Concentrations of elements and total dust are given in grams/area units and month without particle fractionation. Initially, on-site falling dust was collected at five locations, which was expanded to eight locations by June 2020.

Figure 14: Example of a NILU-filter positioned W of Slaggplan.

Table 5 shows the average concentrations measured at the different NILU collectors on-site. These were used as a basis for choosing a location for the monitoring station during this campaign (see section 3.1.2).

Table 5: Average concentrations of Pb and total dust captured by the falling dust collectors at Boliden. Note that Rampen, Filter and Taket measurements started in June 2020, whereas the others started in April 2019. Locations sorted by Pb concentration from high to low.

	Slaggplan	Rampen	Filter	Taket	Reningsverk	Utlastning	Sibirien	G:a utlastningen
Pb [mg/m^2/month]	437	436	415	253	204	131	57	24
Dust [g/m2/month]	8.3	3.8	5.3	3.7	2.8	3.2	2.5	1.7

Three of the falling dust collecting locations have shown particularly high lead concentrations; Slaggplan, Filter and Rampen. In 2021, they accounted for 72% of all lead collected at the site. When including measurements for 2019 and 2020, this percentage decreases to 63%, although both Filter and Rampen were added in June 2020, see Table 6. Filter, the smallest contributor of the three main collectors, accounts for 25% of all lead collected since 2019. After Filter, the "Wastewater treatment" location collected 14% of all dust, which has been active since January 2019.

Table 6: Percentage of all lead measured at the different stations since the measurements started in 2019. Note that Filter-, Ramp- and Roof stations were added in June 2020.

Locations	**2019-2021**	**2020-2021**	**2021**
Group	**63%**	**65%**	**72%**
Slaggplan	48%	37%	38%
Filter	25%	30%	29%
Rampen	27%	33%	33%

Figure 15 shows the seasonal variation in the amount of Pb collected at the three locations with highest concentrations. Although only one complete year of data is available for this group, there seems to be a correlation between the locations, particularly between the Slaggplan and Filter locations.

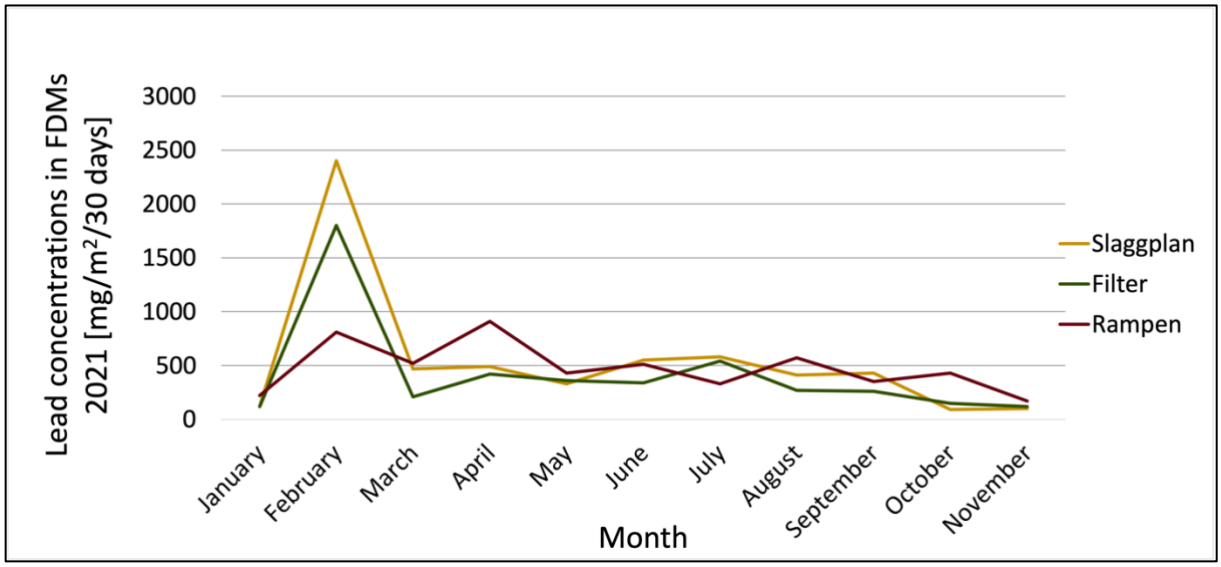

Figure 15: Monthly lead concentrations at the three falling dust stations with the highest recorded concentrations from January to November 2021. Earlier data points were not viable due to the Filter-and Rampen locations being added in June 2020.

Correlation matrices for some of the elements in the FDMs are presented in below. These are based on 32 FDMs, making the critical values for significance 0.35 and 0.45 for p-values of 0.05 and 0.01 respectively. In the subsequent correlation matrices, the correlation coefficients are written in cursive for the first level of significance (0.05) and in bold for the second level of significance (0.01).

The correlation matrix for Slaggplan based on the FDMs is shown in Table 7. As, Fe, Ni, Pb, S and Sb were highly correlated with each other. However, these correlations do not necessarily mean the above elements come from the same source, due to the monthly resolution of the FDMs.

Table 7: Correlation coefficients for elements measured at Slaggplan. Cell colours are attributed accordingly; white < 0.40, 0,40 < yellow < 0,60, 0,60 < blue < 0,80, green > 0,80. Cursive: p < 0.05. Bold: p < 0.01.

Slaggplan											
	As	Ca	Cd	Cr	Cu	Fe	Ni	Pb	S	Sb	Zn
As	1										
Ca	0,24	1									
Cd	0,48	0,72	1								
Cr	0,07	*0,39*	-0,05	1							
Cu	0,56	0,23	0,15	0,48	1						
Fe	0,77	0,21	0,27	0,27	0,59	1					
Ni	0,79	0,22	0,25	*0,42*	0,74	0,84	1				
Pb	0,93	0,07	*0,35*	-0,01	0,55	0,83	0,83	1			
S	0,83	0,45	0,55	0,07	0,58	0,81	0,81	0,87	1		
Sb	0,93	0,12	*0,40*	0,04	0,60	0,81	0,88	0,96	0,87	1	
Zn	0,34	0,19	0,14	0,35	0,57	0,50	*0,43*	0,34	*0,39*	*0,37*	1

The correlation matrix for the FDM location between ScanDust and Boliden is shown in Table 8, titled ScanDust. Note the negative correlations between Pb and Cu, as well as Sb and Cu. In earlier Landskrona measurements, the origin of Cu could not be established, with Boliden, ScanDust and the docks being possible sources (Kristensson, et al., 2019). The negative correlation between Pb and Cu at the Scan Dust location indicates that Boliden should not be the source of Cu, since Pb is the characteristic element of Boliden. Furthermore, the matrix suggests that Sb could be associated with Boliden. It should, however, be noted that the correlations presented are not significant at 0.05 confidence, meaning a correlation between Cu/Pb and Cu/Sb is not statistically proven. Correlations between Sb and Pb were found in the FDMs performed by Landskrona city (Feuk & Weich, 2019).

Table 8: Correlation coefficients for elements measured at Scan Dust. Cell colours are attributed accordingly; red <-0,20, -0,20 < white < 0.40, 0,40 < yellow < 0,60, 0,60 < blue < 0,80, green > 0,80. Cursive: p < 0.05. Bold: p < 0.01.

ScanDust											
	As	Ca	Cd	Cr	Cu	Fe	Ni	Pb	S	Sb	Zn
As	1										
Ca	0,67	1									
Cd	0,75	0,59	1								
Cr	0,64	0,86	0,62	1							
Cu	0,18	0,26	0,20	*0,43*	1						
Fe	0,82	0,80	0,64	0,76	0,20	1					
Ni	0,75	0,84	0,74	0,89	0,30	0,71	1				
Pb	0,33	0,48	*0,44*	*0,43*	-0,28	0,58	*0,44*	1			
S	0,69	0,81	0,56	0,59	0,20	0,62	0,67	0,15	1		
Sb	0,30	*0,38*	0,49	*0,43*	-0,26	0,47	0,48	0,92	0,13	1	
Zn	0,81	0,78	0,60	0,65	0,28	0,68	0,78	0,11	0,79	0,05	1

The high correlation between Sb and Pb is also evident from the Utlastningen correlation matrix in Table 9. Utlastningen is located between the office building and the warehouse on its opposite side (see Figure 7).

Table 9: Correlation coefficients for elements measured at Utlastningen. Cell colours are attributed accordingly; white < 0.40, 0,40 < yellow < 0,60, 0,60 < blue < 0,80, green > 0,80. Cursive: p < 0.05. Bold: p < 0.01.

Utlastningen											
	As	**Ca**	**Cd**	**Cr**	**Cu**	**Fe**	**Ni**	**Pb**	**S**	**Sb**	**Zn**
As	**1**										
Ca	**0,57**	**1**									
Cd	0,27	**0,69**	**1**								
Cr	0,25	0,25	0,10	**1**							
Cu	0,09	*0,36*	0,19	**0,61**	**1**						
Fe	0,27	0,34	0,19	0,22	0,25	**1**					
Ni	0,30	0,25	0,09	**0,98**	**0,56**	0,25	**1**				
Pb	**0,61**	0,30	0,17	0,11	0,07	0,18	0,16	**1**			
S	0,27	*0,35*	0,03	**0,45**	0,30	0,03	**0,49**	0,20	**1**		
Sb	**0,72**	**0,48**	0,32	0,15	0,10	0,25	0,21	**0,93**	0,22	**1**	
Zn	-0,03	0,18	0,03	0,16	0,23	**0,76**	0,19	0,09	-0,05	0,12	**1**

3. Method

3.1. Aerosol sampling

3.1.1. Xact

An Xact 625i Ambient Metals Monitor (further referred to as Xact) was used for measuring airborne metal content. It is an active sampling technology where airborne particles are deposited on a filter tape. Samples are then analyzed automatically by X-ray Fluorescence spectroscopy. The instrument operates on-line, meaning sampling of aerosols is conducted simultaneously as the previous sample is analyzed.

When particles are irradiated by X-ray, they may lose an electron from its inner shells of lower energy. Subsequently, an electron from higher valence shells replaces the lost electron and, in doing so, emits energy of a certain wavelength. This energy can be recorded in a spectrometer. Because each element has its own characteristic fluorescent energy, they can be distinguished from each other (ThermoFisher Scientific, 2020). A picture of the Xact 625i can be seen in Figure 16.

Figure 16: Picture of the Xact 625i Multi Metals Monitor in the lab.

While it has been verified that the Xact produces similar average concentrations as other methods such as inductively coupled plasma methods (Furger et al. 2017), the average daily concentration results from the Xact were intended to be compared to the Particle-Induced X-ray emission (PIXE) results from 24-hour sampling.

The sampling time of the Xact can be set between 15 and 240 minutes. In order to ensure metals, in particular Pb, were above their detection limits, four-hour sampling at the Boliden site was initially applied. This first test-run showed that Pb and many other metals were well above their detection limits, after which sampling times were changed to one-hour sampling and subsequently one-hour sampling. Since Every night at 0:00, the Xact executed a self-calibration protocol which took half an hour. Once this was done, sampling continued at 0:30. This meant the next sample time would be one half hour shorter than the chosen sampling time. Afterwards, the sampling times returned to normal. Figure 17 shows the Xact inside the monitoring station used for the campaign. In order to collect PM_{10} during sampling, a PM_{10} impactor was used and the flow through the pump was set to 16,7 l/min.

Figure 17: View of the Xact monitor inside the cabinet used during the measurement campaign.

3.1.2. Measurement location

According to the falling dust measurements, Slaggplan, Rampen and Filter showed the highest amount of Pb dust accumulation on average. A tour of the entire outside of the facility was held on the 19th of January. Because Slaggplan seemed to be the only location where materials were handled openly in the outside environment, it was deemed a promising site for recording potential spikes in dust concentrations. Furthermore, it was initially assumed that both Rampen and Filter falling dust measurements experienced high concentrations as a result of activity at Slaggplan, since no activities involving open handling of Pb-rich materials could be identified at the former locations.

A monitoring site SE from Slaggplan was chosen (see Figure 18). It was chosen based on the trade-off between distance to Slaggplan and obstruction of traffic at Boliden. It was assumed that W winds would change direction towards SE because of the obstructing building and thus making aerosols from Slaggplan travel towards the monitoring station. This assumption introduces an uncertainty which is discussed in the Results section. Unfortunately, the importance of checking this assumption only became apparent after the measurements. It may have been possible to verify the assumption by setting up anemometers at Slaggplan and the monitoring station.

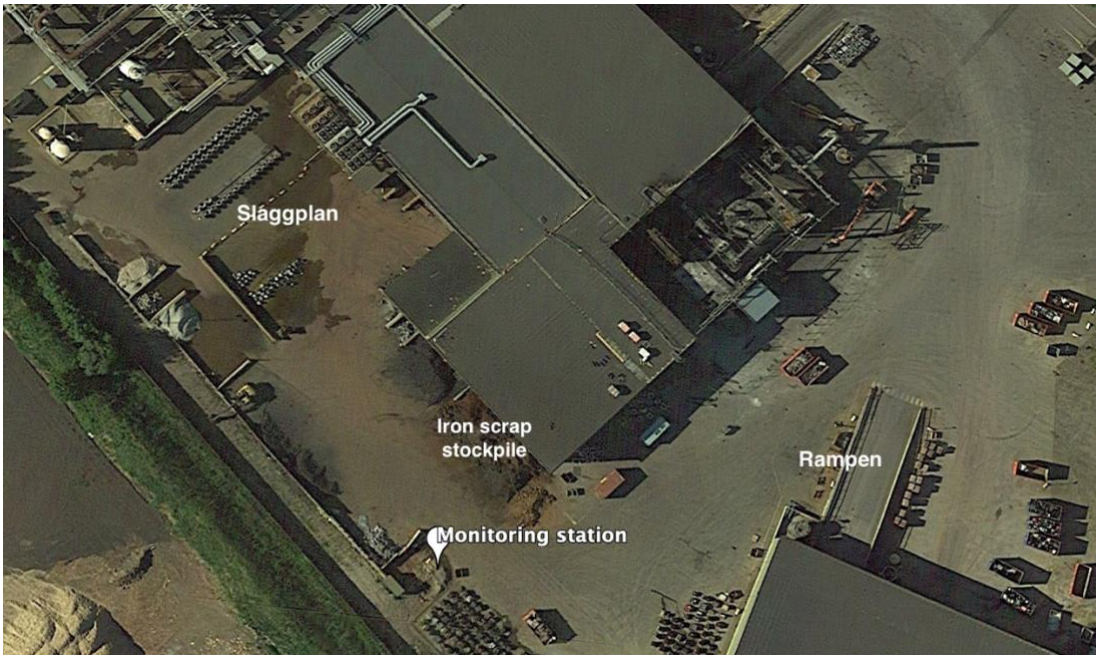

Figure 18: Measurement location in relation to Slaggplan and Rampen.

3.1.3. Instrument setup

In Figure 19 the monitoring station can be seen. The station consisted of a cabinet bolted to a pallet. The gray box on the side is an aggregate for air cooling. This was not used for cooling the cabinet. Instead, a fan on the inside of the cabinet was attached and prevented the temperature in the cabinet from exceeding 18°C. On the side, taped to the AC-aggregate, was a GENT-sampler which was connected to a vacuum pump via blue tubing.

On top of the cabinet, two PM_{10} inlets were connected to tubes which continued inside the cabinet. Both inlets were roughly 2.5 meters above ground. The foremost inlet was attached to the vacuum pump for PIXE filter sampling, until this inlet was exchanged for a GENT sampler. See Appendix A for PIXE method and theory. The backmost tube ran straight through the cabinet roof into the Xact. Two buckets (white) were placed on top of the roof and sealed at the bottom to prevent water from leaking into the monitoring station.

Figure 20, Figure 21 and Figure 22 show the material deposits closest to the monitoring station. The iron and coke stockpiles in Figure 20 were of more granular material than the lead and coke stockpiles in Figure 21 and Figure 22. The surface around the iron lead stockpile show clear signs of rust, indicating the granular structure of the material.

Figure 19: View of the monitoring station.

Figure 20: View towards the material deposits closest to the monitoring station. Coke and iron scrap piles are to the left and right respectively, on the opposite side.

Figure 21: View towards Slaggplan from the monitoring station. The visible pile on the left side also contained coke. A small lead scrap pile was behind the wall to the left and is not visible in the photo.


Figure 22: Picture of the lead scrap pile.

3.2. Temperature and wind data

Temperature and wind data were provided by Boliden. The company had a thermometer and anemometer installed at a high altitude of around 30 meters on a scaffolding. From these instruments, temperature, wind direction and wind speed were measured.

3.3. Measurement period

Once the instrument was transported to the Boliden site, an initial test run of the Xact was conducted between 23rd and 25th of February with four-hour sampling time. This was done to ascertain that the elements of interest, particularly Pb, were detected. This was the case for all sample times during the test period. Two-hour sampling started on the 3rd of March at 12:00 and continued until 8th of March at 12:00. In this period, there was an unexplained shutdown of the sampling after 7:00 on March 4th and the sampling was reactivated the same day at 12:00. After this period, results showed that Pb and a majority of the other elements were above their detection limits. On 8th of March at 14:00, one-hour sampling was initiated. No disruptions were suffered until the end of the sampling campaign on the 13th of March at 22:00. At this point, the filter tape on which samples were collected, had ran out and the replacement filter tape was delayed due to transport issues.

3.4. Logging of activities

In order to investigate a potential relation between elevated PM_{10}-levels and activities at the Boliden site, observations in the outside environment were conducted. From the site description in 2.6, the following activities were deemed worthy of keeping record of:

- traffic in the stockpile corridor, as well as material handling,
- tipping of slag pots at Slaggplan,
- moving of slag blocks by crane and removal of slag by wheel loader and
- surface cleaning by cleaning vehicle, both in the stockpile corridor and at Slaggplan.

The company provided access to live recordings from surveillance cameras with the ability to play back video footage. Figure 23 shows the two areas (Slaggplan and the area between Vågen and Rampen) which were surveilled through the cameras. Unfortunately, cameras were not placed in such a location that observation of traffic in the stockpile corridor was possible. Attempts were made at deducing from both cameras whether a vehicle had passed the material deposits and the monitoring station but the detection range of the second camera did not reach entirely to the other side of the facility. This means it did not register vehicular activity on the west and far-most side of the facility if it did not also register something else. Logging of activities through camera footage was therefore restricted to activities at Slaggplan, including surface cleaning.

Figure 23: Overview of the areas visible from the surveillance cameras, where the blue coloured shape marks the Slaggplan area visible from one camera and the white shape marks the area visible from the other camera. The location of the monitoring station is shown in the figure.

Dumping activities could instead be logged by reviewing documents on departures and arrivals of trailers carrying materials for the stockpiles. When arrival and departure times crossed a sampling point, it was assumed the dumping occurred during the sampling period where the trailer remained for the longest amount of time. For example, if a dumper arrived at 7:53 and departed at 8:01, dumping was assumed to occur on sampling hour 7:00 (for one-hour sampling times).

Regarding the tipping of slag pots, video review of five days showed that pots were tipped several times an hour (between one and five times) during the entire day, with the exception of a four-hour period where no slag pots were emptied. Ultimately, it was decided that this activity was too frequent and continuous each hour to use this data for further inference, considering the minimum sample time was one hour during the measurements.

It should be noted that personnel on-site were informed of this measurement campaign and several of the employees were aware of the authors´ presence in the area. However, since the activities related to the process are continuous and routine-based, any alteration of the activities in order to manipulate the measurement campaign seems unlikely to have occurred.

3.5. Principal Component Analysis

Principal component analysis (PCA) is a multivariate analysis method used for identifying the variables with the most variation in a data set and visualize how they are correlated with one another. The purpose for applying PCA in this work was to see if sources or source categories for airborne particles could be established using this method. For a comprehensive description of the PCA, see e.g. Jolliffe (2002). Below follows a brief explanation of the method.

Each data set consists of p number of variables and m observations. Observations are plotted in a p-dimensional space with each observation being a linear combination of p variables. A linear function $\boldsymbol{a_1x}$ is defined such that the eigenvalue (square distances between the projected

observations on the linear function and the origin) is maximized. The eigenvalue corresponds to the variation in data along the defined linear function.

Equation 1 $$\boldsymbol{\alpha'_1 x} = \alpha_{11}x_1 + \alpha_{12}x_2 + \cdots + \alpha_{1p}x_p = \sum_{j=1}^{p} \alpha_{1j}x_j$$

The linear function in Equation 1 is known as the first *principal component* (PC1). The next principal component will be orthonormal to the prior and have the second highest eigenvalue and variation. This continues until all PCs have been found, which is the same amount as the number of variables *p* (or samples if there are fewer samples than variables). Since PCs are linear combinations of variables, each variable will have a *loading factor* which tells how much a variable contributes to the variation along the PC. Furthermore, eigenvalues of each PC can be compared to find the PCs representing the most variation of the data set. If there are two PCs explaining most of the variation in a data set sample data is conventionally plotted in a 2D-graph with PC1 and PC2 as axes. In the same plot, loading factors of the different variables can be included.

A PCA can be based on either the covariance or correlation matrix of a data set. If there are large differences in variances among the variables, a correlation matrix can be favored because this matrix is standardized, compared to the covariance matrix which contains absolute values for the covariance. To carry out the PCA, the Maths and Statistics toolbox of Matlab was used.

4. Results & Discussion

4.1. Element concentrations

Table 10 shows the average concentrations and standard deviations for the elements measured during the campaign. 15 of the elements sampled are not included in Table 10. It was decided that elements should have been detected at least 85% of the samples to be included in any further analysis. For the elements that did not reach this criterium, see figure B1 in Appendix B. Four elements, Au, Pd, Sb and Mn had not been sampled in earlier aerosol measurements in Landskrona.

Table 10 also includes the same metrics from aerosol measurements in 2003 between 3rd of April and 16th of May at Lundåkrahamnen. This was the year with the highest average concentrations out of the four years that they had been conducted. The average Pb concentration for the Boliden campaign is clearly higher than in previous aerosol measurements in Lundåkrahamnen. Other elements such as Si, S and Cl had higher concentrations during the aerosol campaign of 2003.

Table 10: Average values and standard deviations of elements which passed the detection limits for a minimum of 85% of the samples. Data on previous measurements in Lundåkrahamnen in 2003 between 3rd of April and 16th of May was included for comparison (Kristensson, et al., 2019).

Element	Average [ng/m^3]	Standard deviation	Lundåkrahamnen average April-May 2003 [ng/m^3]
Pb	1464	2104	228
Si	867	637	1635
Fe	830	649	420
S	450	363	1927
Cl	373	534	994
Ca	228	281	710
K	140	84,5	374
Cr	92,8	99,0	8,6
Ni	33,6	33,8	6
Zn	26,3	22,3	46,3
Au	20,8	24,4	-
Pd	19,0	10,2	-
Ti	18,9	18,1	42,7
Sb	16,1	32,5	-
Mn	12,4	11,2	15
Mo	12,2	16,4	-
Cu	10,7	13,4	10,8
Sr	0,83	1,04	5,6

Average composition of the aerosols measured in the Boliden campaign are presented in Figure 24. The relative contributions of Pb, Fe, Si, S, Cl, Ca, and K in the Lundåkra campaign of 2003 are also included for comparison. The larger contribution by Pb to the total element concentration (TEC) in the Boliden campaign is evident (22% of total TEC compared to 3% relative to the element selection). Note that lighter and abundant elements such as oxygen were not capable of being detected by the Xact, meaning the average contributions below do not represent the true element contributions to the TEC. This should also be considered whenever TEC is referred to in subsequent paragraphs.

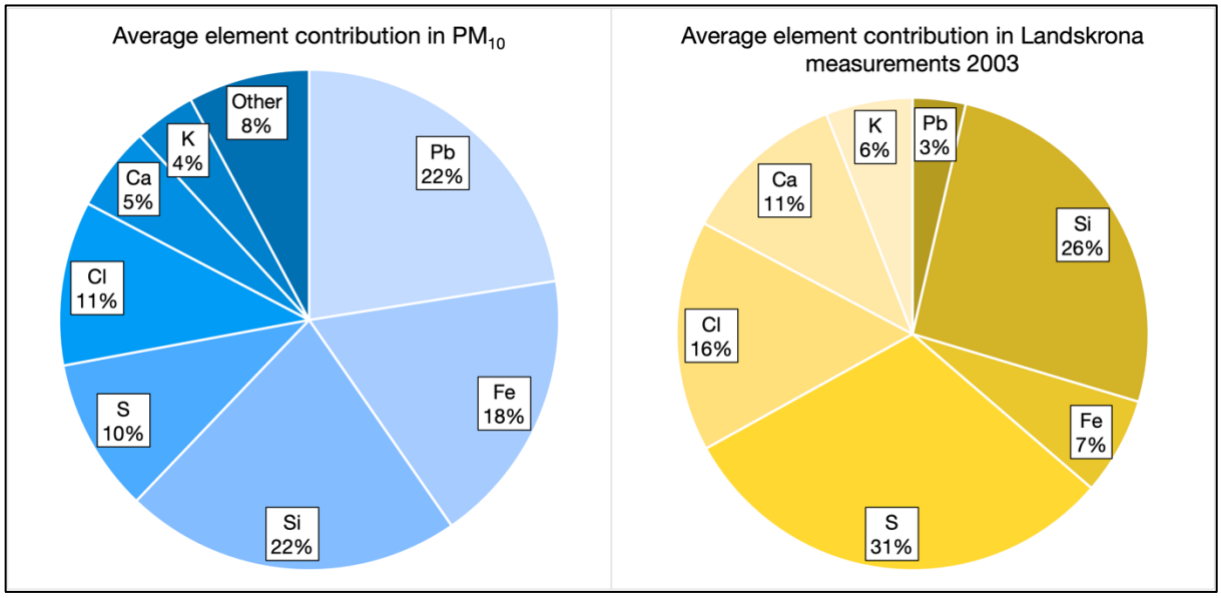

Figure 24: Average element contributions for the Boliden campaign (left) and Lundåkra 2003 campaign (right). The fine and coarse fractions from the Lundåkra campaign were summed together before calculating average compositions. It is important to note that the right pie-chart only shows the relative contribution between the chosen elements, since no category equivalent to "Other" exists in this chart.

The average daily Pb concentrations were between 1 and 2 µg/m^3 and are shown in Figure 25. Weekends spanned across 5th-6th and 12th-13th of March. The time series of eight days was too small for robust statistical inference regarding differences in weekday and weekend concentrations. However, the data indicates they are similar. Observations showed that activities at Slaggplan continued at the same pace throughout the week. Weekends differed in that the otherwise busy traffic by Vågen and surface cleaning did not occur. This indicated that the traffic by Vågen and the surface cleaning vehicle did not have a considerable effect on the measured concentrations.

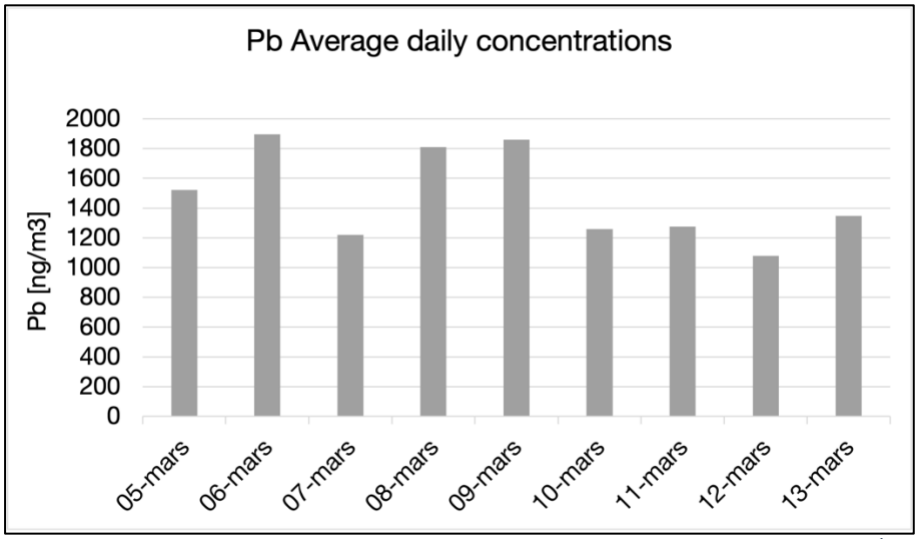

Figure 25: Average lead concentrations for each day of Pb sampling. One hour of data is missing on the 8th of March between hours 13-14 and on the 13th of March between hours 23-0. 3rd and 4th of March were omitted; 12 and 4 hours of data respectively were missing.

The temporal variation in total element concentration TEC during the measurement campaign is shown in Figure 26, where the percentage contribution of the seven most abundant elements, Pb, Fe, Si, S, Cl, Ca, and K, are plotted individually and other elements are aggregated as

"Other". The individually plotted elements accounted for a majority of the total element concentration throughout the campaign.

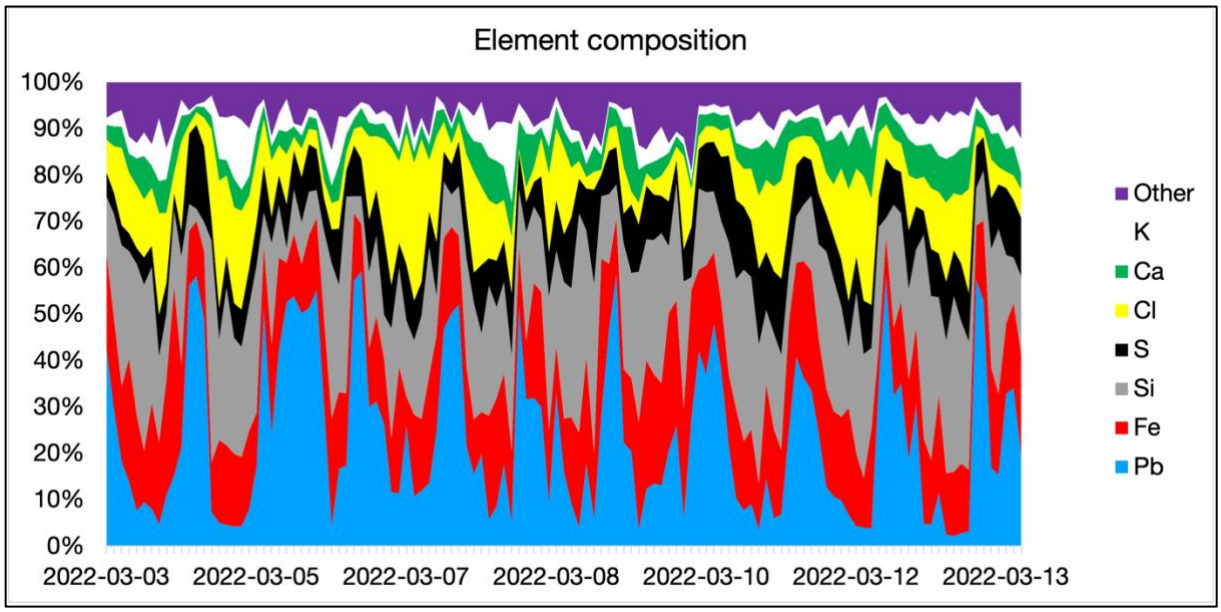

Figure 26: Total element composition during the measurement campaign. 2-hour averages were applied for the graph to smoothen it out. The change in scale on the time axis after 8th of March is due to sampling time being reduced from two hours to one hour.

The Pb concentrations followed a day-night cycle with higher concentrations during the day compared to night time. Diurnal concentrations of Pb are shown in Figure 27. For diurnal concentrations of other elements, see figure C1-C4 in Appendix C.

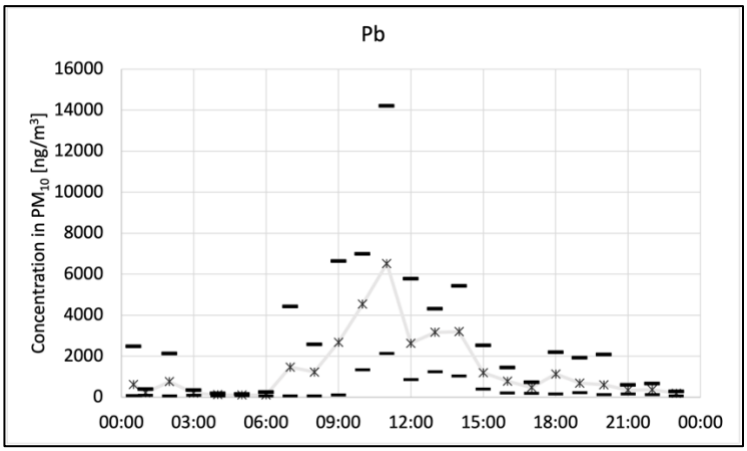

Figure 27: Diurnal concentration of Pb. Crosses represent average concentrations. Bars above and below the crosses represent maximum and minimum concentrations respectively.

Although Pb had the highest average concentration, its background concentration during night hours is comparable to that of Si, Fe and S as shown in Figure 28 below. Day-night cycle behaviour is also evident among Fe and S, although not as distinctly as for Pb.

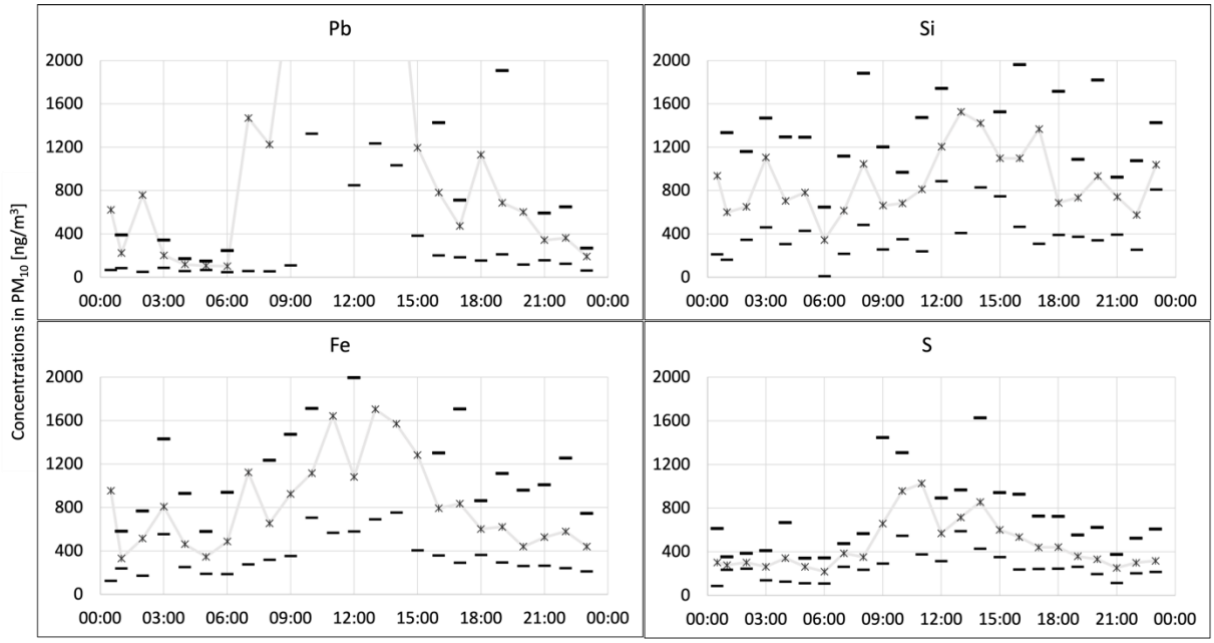

Figure 28: Diurnal concentrations for Pb, Si, Fe and S. Crosses represent average concentrations. Bars above and below the crosses represent maximum and minimum concentrations respectively.

In Figure 29, TEC- and Pb concentrations are plotted together. The two series correlate well with each other. Since Pb seemed to be the main component of TEC during peak hours and Boliden has been shown to be the source of Pb, this element was chosen as an indicator for investigating whether activities at Boliden were causing diffuse dust emissions. This was also advantageous since background concentrations of Pb were much lower than their peak concentrations, compared to the other elements with relatively high concentrations.

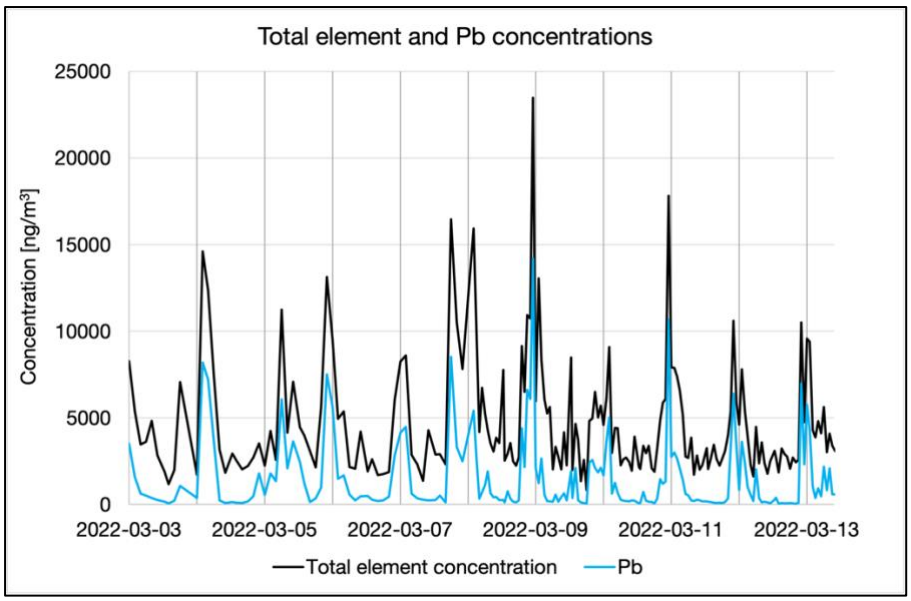

Figure 29: Total element and Pb concentrations in ng/m^3. Each vertical line is positioned at 12:00 for each day.

shows the correlation matrix for 12 of the elements in Table 10, as well as for the total element concentration (TEC). Significance of 0.05 and 0.01 are indicated by cursive and bold formatting respectively. The total number of samples was 187 with the critical values being 0.15 and 0.19 for 0.05 and 0.01 confidence levels respectively. In accordance with previous measurements, the correlation coefficient between Pb and Sb was high (0.74). Pb was also correlated with Fe and S with correlation coefficients of 0.61 and 0.81 respectively. If Fe, S and Sb would have

originated primarily from background sources, their correlations with Pb would have been comparable to the correlations between Pb and other elements linked to earth dust such as Ca and Si (0.32 and 0.07 respectively). Instead, the higher correlation coefficient between Pb and Fe, S and Sb indicate that these elements originate from Boliden. Fe differs from the rest, however, in that correlation coefficients between Pb, S and Sb with Si were low (maximum of 0.18 between S and Si), whereas the correlation coefficient between Fe and Si was 0.47. This suggested a considerable amount of Fe might have originated from earth dust or other sources. This was confirmed by the results from the PCA, described hereafter.

Table 11: Correlation matrix for the Boliden campaign. Out of the 18 elements passing the sample detection criterium of 85%, 12 elements are presented here, including the total metal concentration. The remaining elements were omitted due space limitations. Cell colours are attributed accordingly; white < 0.40, 0,40 < yellow < 0,60, 0,60 < blue < 0,80, green > 0,80.

	TEC	Si	S	Cl	K	Ca	Ti	Cr	Mn	Fe	Ni	Mo	Sb	Pb
TEC	1													
Si	0,41	1												
S	0,83	0,18	1											
Cl	0,24	0,18	0,11	1										
K	0,23	0,41	0,13	0,12	1									
Ca	0,53	0,53	0,43	0,19	0,60	1								
Ti	0,42	0,49	0,32	0,06	0,40	0,63	1							
Cr	0,23	0,30	0,02	-0,02	-0,08	-0,05	0,01	1						
Mn	0,60	0,59	0,32	0,17	0,46	0,61	0,48	0,57	1					
Fe	0,81	0,47	0,55	0,16	0,14	0,39	0,38	0,59	0,80	1				
Ni	0,22	0,29	0,00	-0,02	-0,09	-0,06	0,00	0,99	0,57	0,58	1			
Mo	0,22	0,25	0,01	0,05	-0,09	-0,09	-0,02	0,93	0,55	0,54	0,94	1		
Sb	0,67	0,06	0,64	0,04	0,02	0,21	0,17	-0,01	0,16	0,42	-0,02	0,00	1	
Pb	0,92	0,07	0,81	0,12	0,06	0,32	0,24	0,04	0,32	0,61	0,03	0,05	0,74	1

Only the first six elements from Table 10 were included in the data set for the PCA. Already at K, the seventh element, the ratio between the standard deviation of Pb and K was 25:1. Adding more elements to the PCA had practically no effect other than making it difficult to discern the loading factors of the elements with most variability. When applying the covariance matrix for the PCA, the two first PCs explained 97% of all variation in the data set, as can be seen in the scree plot in Figure 30. Thus, a PCA with two principal components was sufficient for illustrating the variability of the data set in a biplot.

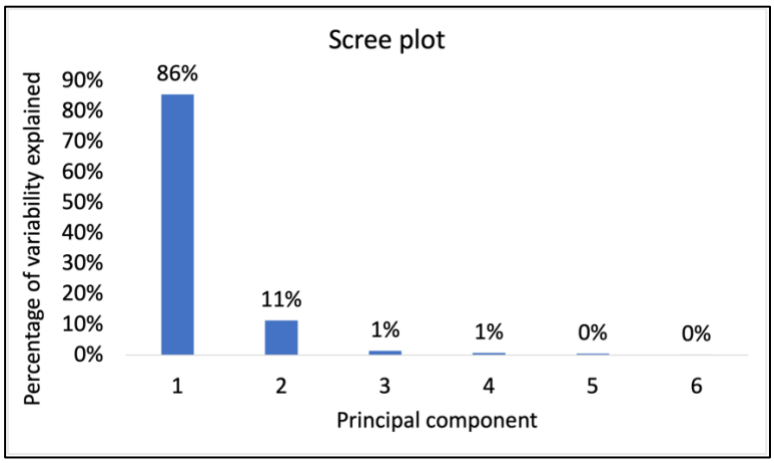

Figure 30: Scree plot for the correlation-based PCA of the trimmed data set. Principal components 1 and 2 explain 97% of the total variation.

The first and second components explained 86% and 11% of the total variability respectively among the six elements (Pb, Si, Fe, Cl, S and Ca). The loading factors of these elements are shown in the biplot in Figure 31, except for Ca which was not visible. Component 1 was dominated by Pb, due to its variability being the highest. Si, Fe, S and Cl were part of Component 1 as well. On the other hand, all other elements than Pb were present in Component 2. This confirms the previous hypothesis that Fe had other sources, which also turned out to the case for the other elements in Component 2. However, since only 11% of the total variability was explained by Component 2, the dominant source for at least Fe and S would likely have come from Boliden. Otherwise, the correlation between Pb/Fe and Pb/S would presumably have been lower.

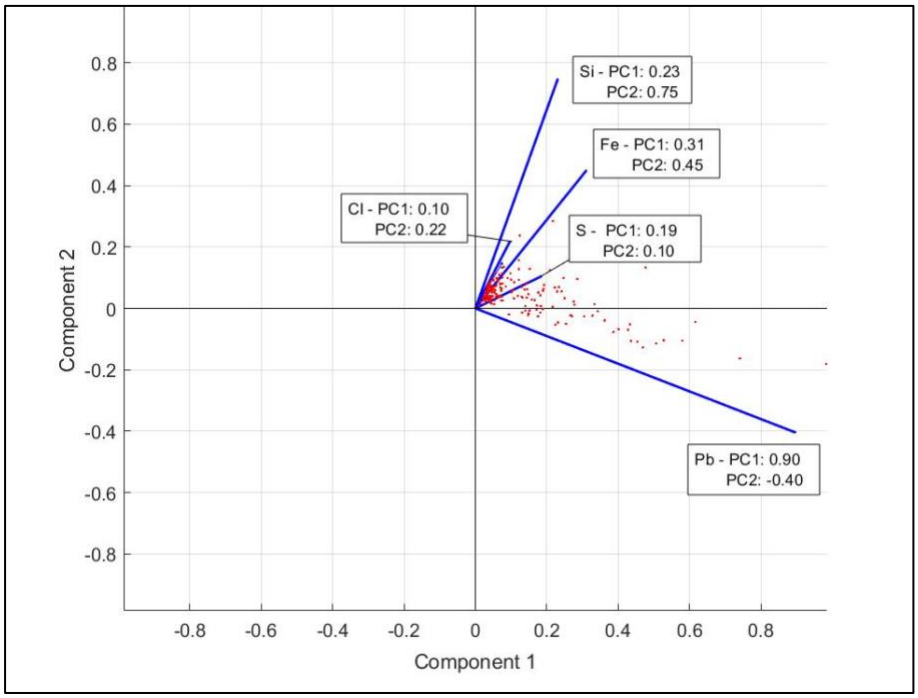

Figure 31: Results from the PCA illustrated in a biplot. Red dots are observations decomposed on the principal components. Blue lines show loading factors for the elements contributing most to the variability.

Since Pb, S and Sb correlated well with each other, an attempt was made at establishing the origin material of the aerosols containing these elements. The ratios between the concentrations of Pb/Sb and Pb/S are shown in Figure 32 as cumulative distribution functions. In 71% of the samples, Pb concentration (Pb-C) was 60 times higher than the Sb concentration (Sb-C). In

46% of the samples, Pb/S exceeded 2, whereas in 33% of the samples, Pb/S was less than or equal to 1. These latter samples reflect the night time conditions since the background concentration of Pb was lower than that of S during night time.

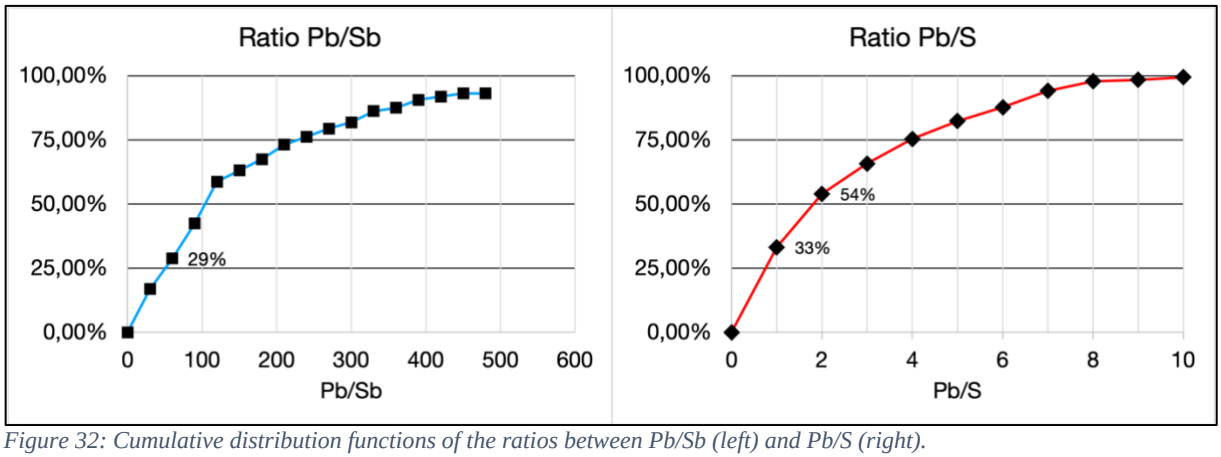

Figure 32: Cumulative distribution functions of the ratios between Pb/Sb (left) and Pb/S (right).

Considering the ratios between Pb, Sb and S, only the lead paste and filter dust could reasonably represent sources for these elements (described in Section 2.6.1). The other known material compositions for materials handled outside are those of the slag and the matte but these materials both have higher contents of S than Pb. The difference in concentration between Pb and S in the matte was too high to suspect it of being the origin of Pb, S and Sb. The ratio between Pb and S is higher in slag than matte and could potentially have been the common source. However, slag mostly contained Fe and Si and if slag was the common source for Pb, Sb and S, the former concentrations would be expected to surpass Pb-C during peak hours. The relationship between slag handling and Pb-C is further investigated in the next section.

4.2. Diffuse lead emission mechanisms

One of the purposes of this campaign was to understand the mechanism/s behind the diffuse dust emissions occurring at Boliden. The diurnal trend of the Pb concentration (Pb-C) indicates that resuspension might have been the main mechanism by which aerosols became airborne at the facility. In this case, deposition of Pb on the ground would have been favoured over suspension during night time. Pb-C is plotted with temperature and relative humidity in Figure 33. The fact that air humidity was higher during night time means surfaces were more likely to be damp, supporting the resuspension theory. Afterwards, during the day, gradual heating of the ground would have allowed for deposited material to suspend. The large peaks observed could therefore possibly be the result of suspension of the accumulated layer of particles on the ground. According to Figure 33, somewhat disagreeable with the resuspension theory, Pb-C sometimes increased before the ambient temperature was above freezing. However, this might be explained by a difference in ground and ambient temperature during the morning hours after sunrise.

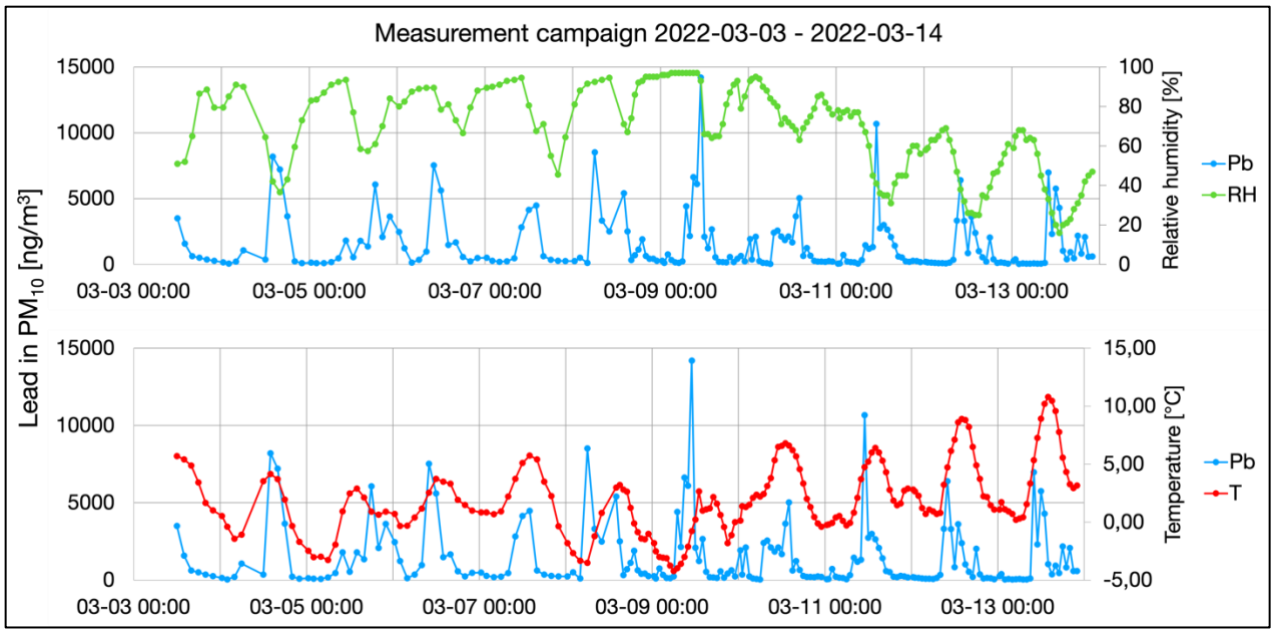

Figure 33: Lead in PM_{10} plotted with relative humidity (above) and temperature (below). Note that sampling time was changed from two hours to one hour on March 8th and that the abruption in measurements between 13:00 and 14:00 on this day is not visible in the graph.

Activities relating to the handling of slag at Slaggplan are plotted with Pb-C in Figure 34. Note that slag handling was continuous throughout the day and night. Furthermore, wind speed and direction are plotted with Pb-C in Figure 35. As discussed in 3.1.2, W winds were assumed to turn at the process facility, transporting aerosols towards the monitoring station. However, wind direction and speed should preferably have been measured to verify this assumption.

Sometimes, slag-handling activities coincided with peaks in Pb-C. This happened on six (6th, 7th, 8th, 9th, 10th and 12th) of the nine days between March 5th-13th. For expanded graphs over these activities and Pb-C for the measurement period, see figure D1 in Appendix D. Four days, the peak occurred with slag moving and removing in the same sample time. Surface cleaning was done in conjunction with the largest peak on the 9th. Note that W winds were prevailing during the first half of the campaign from the 5th at 12:00 and 9th at 0:00. On the 9th and onward, SE winds dominated throughout the campaign. Regardless if the assumption about the trajectory of W winds was true, peaks in Pb occurring on the 10th and 12th should not be attributable to the registered activities during those peak hours.

Although slag-handling activities and surface cleaning did coincide with peaks in Pb-C on the occasions described above, there were several times where these activities occurred during episodes with little or no elevation in Pb-C compared to its background levels, even during W winds. This was particularly the case during night time. A longer time-series with higher temporal sample resolution would be beneficial for isolating the potential emissions from the slag-handling activities and surface cleaning events. Based on the results from this study, contributions from these activities to airborne Pb will be considered minor compared to the contribution from lead paste and/or filter dust in the outside environment.

The peaks usually coincided with an increase in wind speed. It should however be noted that wind speed increased most days with a simultaneous increase in temperature. As mentioned, the moisture content of the ground must be reduced to a minimum before dust can resuspend, making temperature a seemingly more important factor than wind speed, at least in terms of when a resuspension episode begins. The overall effect of wind speed on the average daily

concentrations is unknown since there were mainly two conditions during the campaign; predominantly W winds with low (2-4 m/s) wind speeds during the first half of the campaign and predominantly SE wind with high (5-8 m/s) wind speeds during the second half of the campaign. A larger data set with more variation in wind speed and direction would be necessary to draw any conclusions regarding the effect of wind speed on Pb-C.

The spikes in Pb-C on the night of the 10th may be explained by a simultaneous increase in temperature and wind speed, as well as decrease in relative humidity. It is likely that some dust suspended during the night under these conditions, as these factors favour suspension. Compared to the daytime peaks, peaks at night were relatively small and did not contribute much to the daily average Pb levels. After some nights with peaks in concentration, presumably as a result of resuspension from the ground, the peak at daytime appears to be smaller than other observed days. This could be due to some particles already having left the ground at night, according to the resuspension theory.

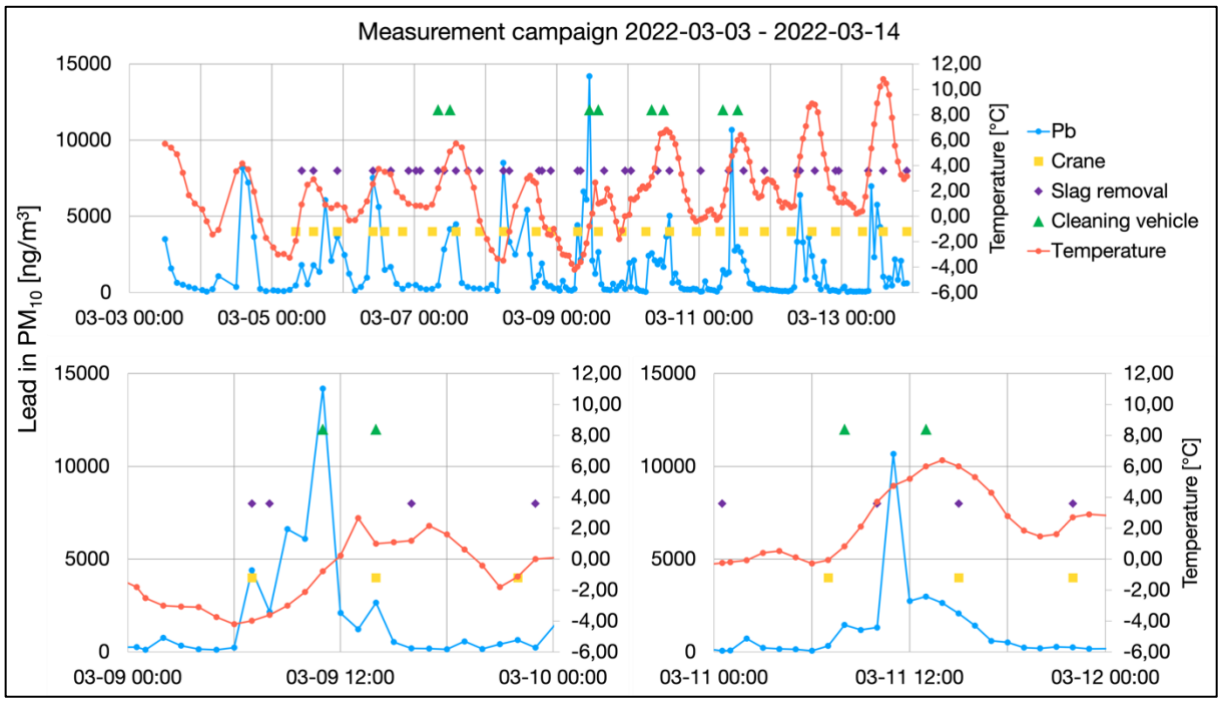

Figure 34: Lead in PM_{10} plotted against temperature for the whole measurement campaign (above) and for the 9th and 11th of March respectively (below). Activities described in section 3.4 are included by the time of their occurrence within a time interval matching the sampling time of the Xact. Note that sampling time was changed from two hours to one hour on March 8th and that the abruption in measurements between 13:00 and 14:00 on this day is not visible in the graph. Activities registered at the site this hour are not included in the graph.

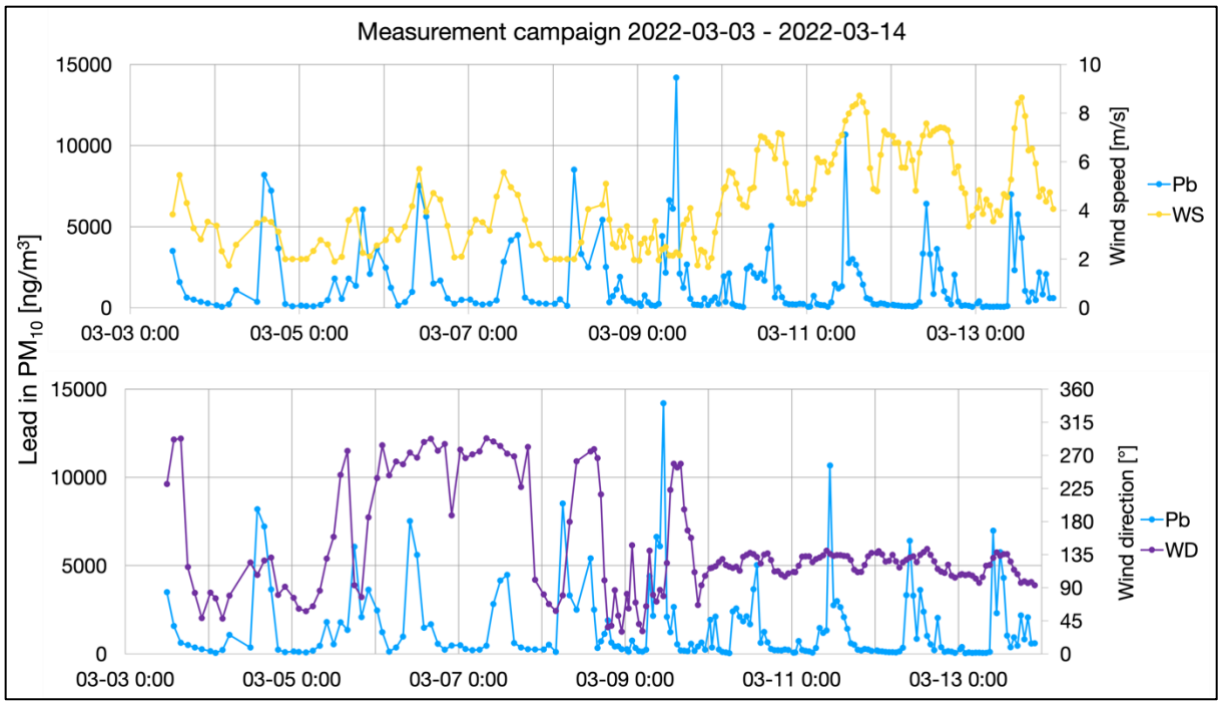

Figure 35: Lead in PM_{10} plotted against time with wind speed (above) and wind direction (below). 0°!/360° in the lower graph represents N, 90° represents E and so on. Note that sampling time was changed from two hours to one hour on March 8th and that the abruption in measurements between 13:00 and 14:00 on this day is not visible in the graph.

As mentioned in 2.6, the monitoring station was close to material deposits of lead and iron scrap, as well as coke. Dumping of such material occurred on eight occasions, seven of which are presented in Figure 36 with Pb-C. The first Pb-C peaks on the 8th and 10th (during the day) differ from other peaks in that they occurred immediately before any moderate elevation of Pb-C. Since Pb-C spiked even though Pb would not have been present in the dumped material on the 8th (casting coke), dumping might have caused suspension of particles present on the nearby ground.

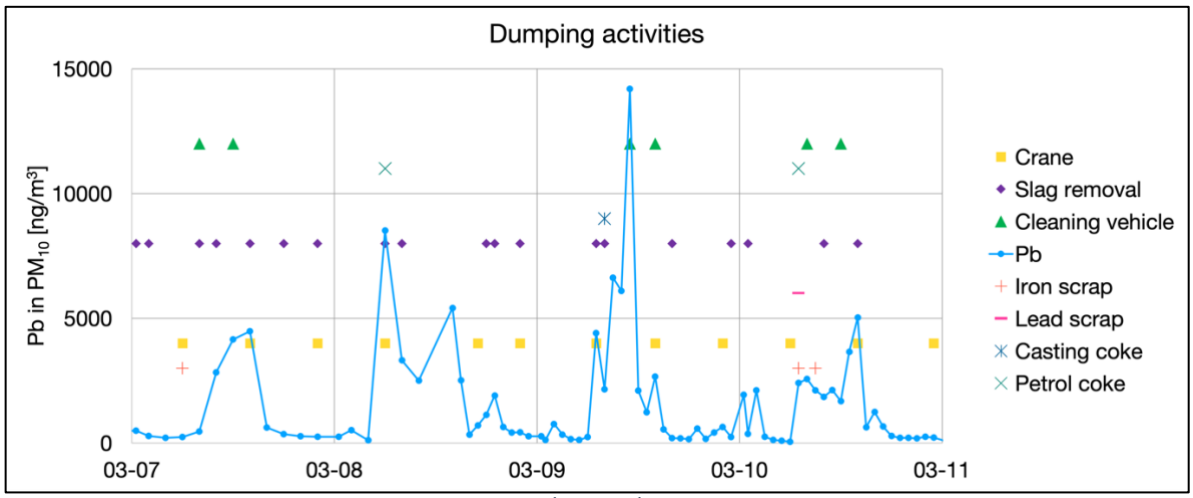

Figure 36: Lead concentrations and activities between 7th and 11th of March. Dumping activities are included, represented by the four last items in the legend.

Resuspension of particles could have more causes than described thus far in this section. It is difficult to establish what mechanical forces contributed most to resuspension, e.g. wind-, traffic- or dumping activities. The absolute wind speed did not seem to affect the average concentration of Pb in PM_{10} according to Figure 35, where the wind speed was higher during the second half of the campaign. This was in line with the theory on wind resuspension

presented by Nicholson (1993). However, wind, traffic and dumping could all have contributed to resuspension of deposited material. The traffic volume was, as mentioned earlier, unfortunately not assessed during the campaign. It would particularly have been worth logging how often vehicles with potential dust slurry on their wheels travelled close to the monitoring station, assuming dust from inside the facilities was the main origin of Pb. There are also other factors, which were not investigated, that could have affected resuspension. For example, different ground areas could have dried up during different times of the day due to shading. Another factor could be the large basin of water, described in 2.6, which existed throughout the campaign. Particles may have been spread to the surrounding surfaces by vehicles travelling through it, with entailing suspension once the particles dried. Considering this last possibility, it might be interesting for further studies to analyse its contents.

Although airborne Pb seems to originate from lead paste or filter dust found inside the process facilities, dust clouds were visible at Slaggplan, during e.g. slag removal, and during material dumping. If these activities are to be studied further, other methods traditionally used for measuring diffuse dust, such as those described in 2.2, might be applied. Particularly, higher temporal resolution of seconds or minutes would be necessary to isolate short bursts of emissions. Dust emissions from traffic could also preferably be measured using higher-temporal resolution.

It should be noted that the concentration results from the Xact have not yet been verified against other methods. The daily collection of particles by the Xact were intended to be compared to that of filters collected for PIXE analysis. The PIXE method and theory are presented in Appendix A. Unfortunately, the PIXE analysis was not completed within the time frame of this thesis. Due to instrument and handling errors, only a few filters were collected for PIXE analysis during the measurement period. It was furthermore not possible to analyse these filters due to the PIXE equipment being unavailable after samples had been gathered.

5. Conclusions

The results from this work suggests that Pb is the main constituent of the aerosols that were assessed at Boliden and that suspension of lead paste during the daytime is likely the main mechanism by which aerosols become airborne, after it has been spread out by vehicles travelling in and out of the processing facility. It was concluded that slag handling activities at Slaggplan were not likely the main origin of the aerosol particles, as was otherwise hypothesized at the onset of this work. This is based on the assumption that wind moved sufficiently from Slaggplan to the monitoring station during W winds.

Measurements could have benefited from acquiring more concentration data over a longer period of time and verification of measurements using PIXE analysis. Furthermore, other data regarding traffic patterns in the stockpile corridor could have given more insight into the role of traffic on suspension of dust at Boliden. The quality of the analysis would also have increased if wind direction and speed had been measured closer to the monitoring station. This would have increased the understanding of the wind movement in the area, where buildings and other obstacles might have caused the wind directions and speeds measured in this work to deviate from the wind directions and speeds through the stockpile corridor to the monitoring station.

Since suspension of lead paste was hypothesized to be the main mechanism for spreading of aerosols, actions directed towards managing the surfaces at Boliden are recommended. There appeared to be no difference in average daily Pb concentration whether surface cleaning was conducted or not. Therefore, it is not possible to attribute surface cleaning with neither positive or negative effects with regards to the spreading of diffuse dust. Absence of surface cleaning, however, might result in more build-up of dust over time which could eventually be spread out by resuspension.

While the efficacy of the surface cleaning method remains uncertain, preventive action towards minimizing diffuse dust sources is perhaps the most suitable strategy for handling the issue. Efforts may be directed at reducing the amount of dust slurry escaping the processing facilities, for example by not allowing vehicles inside the facilities to enter the outside environment without first being cleaned. Additionally, the capacity for the water basin at Slaggplan to act as a point of accumulation of metals should be investigated. If this basin is rich in metals, its location could prove a potent emission source if it dries up during long periods of warm weather with no rain.

Future measures for mitigating diffuse dust emissions at Boliden should be coupled with measurements before and after implementation to allow for evaluation of mitigation strategies. However, due to the seasonal variation in diffuse dust emissions, it may be difficult to evaluate the efficiencies of corrective measures with lower temporal resolution. Thusly, using the Xact metals monitor would also be beneficial in the future due to its temporal resolution being higher. On the other hand, the ongoing falling dust measurements should also show long-term decrease in Pb concentrations if efficient measures are applied at Boliden. A combination of measurements with high- and low temporal resolution may thus be optimal for evaluating mitigation strategies.

References

Directive 2008/50/EC of the European Parliament and of the Council of 21 May 2008 on ambient air quality and cleaner air for Europe. (2008). *Official Journal*(L152), p. 1.

Befesa ScanDust. (n.d.). *Om Befesa ScanDust*. Retrieved 03-01 2022, from https://scandust.se/om-befesa-scandust/

Berger, C. S., Berger, L., & Skerratt, L. F. (2019). Airborne lead dust concentration in Townsville, Queensland is associated with port activity and may contribute to estuarine sediment contamination. *Estuarine, Coastal and Shelf Science 225*.

Farago, M., Thornton, I., White, N., Tell, I., & Mårtensson, M.-B. (1999). Environmental Impacts of a Secondary Lead Smelter in Landskrona, Southern Sweden. *Environmental Geochemistry and Health volume, 21*, pp. 67-82.

Feuk, E., & Weich, R. (2019). *Mätningar av tungmetaller i fallande stoft i Landskrona 2018.* Landskrona: Landskrona stad Miljöförvaltningen.

Genaidy, A. M., Sequeira, R., Tolaymat, T., Kohler, J., & Rinder, M. (2009). Evidence-based integrated environmental solutions for secondary lead smelters: Pollution prevention and waste minimization technologies and practices. *Science of the Total Environment*, pp. 3239-3268.

Gustafsson, M., & Petersson, K. (2016). *Diffusa partikelemissioner från Vargön Alloys.* Stockholm: Svenska Miljöinstitutet.

Gustafsson, M., Blomqvist, G., Johansson, C., & Norman, M. (2012). *Driftåtgärder mot PM10 på Hornsgatan och Sveavägen i Stockholm.* Linköping: VTI.

Gustafsson, M., Saucedo, V. G., Rosendahl, S., & Lindén, J. (2020). *Guide till damningsreducerande åtgärder.* Stockholm: IVL Svenska Miljöinstitutet.

Haeger-Eugensson, M., Achberger, C., & Jacobsson, N. (2015). *Uppskattning av diffus damning av bly från Boliden Bergsöe.* Göteborg: COWI.

Hinds, W. (1999). *Aerosol Technology: Properties, Behavior, and Measurement of Airborne Particles.* New York: John Wiley Sons Inc.

Jolliffe, I. T. (2002). *Principal Component Analysis* (Vol. 2). Aberdeen, United Kingdom: Springer.

Kok, J. F., Parteli, E. J., Michaels, T. I., & Karam, D. B. (2012). The physics of wind-blown sand and dust. *Reports on Progress in Physics, 75*, p. 2.

Kristensson, A., Prosper, W., Pallon, J., Feuk, E., Alikioti, D., & Nilsson, P. (2019). *Metaller i luftburna partiklar i Landskrona 2017.* LTH, Avdelningen för kärnfysik. Lunds Universitet.

Landskrona stad. (2021, 03 11). *Blyhalter i blod*. Retrieved 03-01 2022, from https://landskrona.miljobarometern.se/miljo-och-halsa/bly-i-blod-hos-barn/blyhalter-i-blod/

Livsmedelsverket. (2022, January 11). *Bly*. Retrieved February 2022, from https://www.livsmedelsverket.se/livsmedel-och-innehall/oonskade-amnen/metaller1/bly

Mallone, S., Stafoggia, M., Faustini, A., Gobbi, G., Marconi, A., & Forastiere, F. (2011). Saharan Dust and Associations between Particulate Matter and Daily Mortality in Rome, Italy. *Environmental Health Perspectives*, *119*(10), pp. 1409-1414.

Martín, F., Pujadas, M., Artinano, B., Gómes-Moreno, F., Palomino, I., Moreno, N., . . . Guerra, A. (2007). Estimates of atmospheric particle emissions from bulk handling of dusty materials in Spanish Harbours. *Atmospheric Environment 41*, pp. 6356-6365.

MMD 1205-13 (Mark- och Miljööverdomstolen).

Nicholson, K. W. (1993). Wind-tunnel expirements on the resuspension of particulate material. *Atmospheric Environment, 27A*(2), pp. 181-188.

Nicholson, K. W. (2009). The dispersion, deposition and resuspension of atmospheric contamination in the outdoor urban environment. *Radioactivity in the Environment, 15*, pp. 22-53.

Nickling, W. G., & Neuman, C. K. (2009). Aeolian Sediment Transport. In A. J. Parsons , & A. D. Abrahams, *Geomorphology of Desert Environments* (Vol. 2). Dordrecht, Netherlands: Springer.

Organization, W. H. (1999). Chapter 7 - Wet Methods. In *Hazard Prevention and Control in the Work Environment: Airborne Dust* (p. Chapter 6). WHO.

Poortinga , A., van Minnen, J., Keijsers, J., Riksen, M., Goossens, D., & Seeger, M. (2013, 09 18). *Measuring Fast-Temporal Sediment Fluxes with an Analogue Acoustic Sensor: A Wind Tunnel Study.* Retrieved 05 2022, from PLOS ONE: https://journals.plos.org/plosone/article?id=10.1371/journal.pone.0074007

Prosper, W. (2017). *The Metal Content in Airborne Particles in Landskrona.* Department of Nuclear Physics. Lund: Lund University.

Rubin, R., & Strayer, D. (2008). Environmental and Nutritional pathology. In *Rubins pathology; Clinicopathologic Foundations of Medicine. 5th ed.* Lippincot Williams & Wilkins.

Sina, H., Sowlat, M., Pakbin, P., Katzenstein, A., & Low, J. (2020, October). High time-resolution and time-integrated measurements of particulate metals and elements in an environmental justice community within the Los Angeles Basin: Spatio-temporal trends and source apportionment. *Atmospheric Environment: X, 7*(100089).

Stempniewicz, M. M., Zhipeng, C., Yanhua, Z., & Komen, E. M. (2018). Resuspension models for monolayer and multilayer deposits of graphite dust. *Annals of Nuclear Energy, 120*, pp. 186-197.

Strömberg, M. (2022, 02 25). Intervju med Mårten Strömberg - Miljöchef på Boliden Bergsöe. (M. Norlin, Interviewer)

Strömberg, U., Lundh,, T., & Skerfving, S. (2008). Yearly measurements of blood lead in Swedish children since 1978: The declining trend continues in the petrol-lead-free period 1995– 2007. *Environmental Research, 107*(3), pp. 332-335.

Stroh, E., Lundh, T., Oudin, A., Skerfving, S., & Strömberg, U. (2009). Geographical patterns in blood lead in relation to industrial emissions and traffic in Swedish children, 1978–2007. *BMC Public Health, 9*, p. 225.

ThermoFisher Scientific. (2020, January 28). Retrieved February 2022, from What is X-ray Fluorescence (XRF) and How Does it Work?: https://www.thermofisher.com/blog/ask-a-scientist/what-is-xrf-x-ray-fluorescence-and-how-does-it-work/

US EPA. (1986). *12.11 Secondary Lead Processing: Final Section - October 1986.* Retrieved from AP 42, Fifth Edition, Volume I, Chapter 12: Metallurgical Industry: https://www.epa.gov/air-emissions-factors-and-quantification/ap-42-fifth-edition-volume-i-chapter-12-metallurgical-0

Wani, A., Ara, A., & Usmani, J. (2015). Lead toxicity: a review. *Interdiscip Toxicol, 8*(2), pp. 55-64.

World Health Organization. (1999, April 8). *Hazard prevention and control in the work environment : airborne dust.* Retrieved 03 2022, from World Health Organization: https://apps.who.int/iris/handle/10665/66147

World Health Organization. (2000). *WHO Air Quality Guidelines for Europe, Second Edition*. Retrieved 02 9, 2022, from Euro.who.int: https://www.euro.who.int/__data/assets/pdf_file/0020/123077/AQG2ndEd_6_7Lead.pdf

World Health Organization. (2003). *Health aspects of air pollution with particulate matter, ozone and nitrogen dioxide.* Report on a WHO working group, Bonn, Germany 13–15 January 2003 . Copenhagen: WHO Regional Office for Europe.

World Health Organization. (2006). *Health risks of particulate matter from long-range transboundary air pollution.* Regional Office for Europe & Joint WHO/Convention Task Force on the Health Aspects of Air. Copenhagen: WHO Regional Office for Europe.

World Health Organization. (2007). *Health risks of heavy metals from long range transboundary air pollution.* Retrieved from https://www.euro.who.int/en/publications/abstracts/health-risks-of-heavy-metals-from-long-range-transboundary-air-pollution-2007#:~:text=Heavy%20metals%20are%20associated%20to,and%20potentially%20even%20lung%20cancer.

World Health Organization. (2021). *Ambient (outdoor) air pollution*. Retrieved February 2022, from World Health Organization: https://www.who.int/news-room/fact-sheets/detail/ambient-(outdoor)-air-quality-and-health

World Health Organization. (2021). *WHO global air quality guidelines. Particulate matter (PM2.5 and PM10), ozone, nitrogen dioxide, sulfur dioxide and carbon monoxide. Executive summary.* Geneva: World Health Organization.

Xing, W., Yang, H., Ippolito, J. A., Zhao, Q., Zhang, Y., Scheckel, K. G., & Li, L. (2020). Atmospheric deposition of arsenic, cadmium, copper, lead and zinc near an operating and an abandoned lead smelter. *Journal of Atmospheric Quality*, pp. 1667-1678.

Appendix A – Particle-induced X-ray emission

Particle-induced X-ray emission (PIXE) is a method of analysing elements by a characteristic x-ray emission. A proton beam is used to excite the inner shell electrons of an atom which leaves vacancies in the inner shell. The vacancies are filled by electrons from an outer shell which creates a characteristic X-ray emission. The emission has a certain energy depending on the energy differences between the inner and outer shells and the intensity is proportional to the concentration. PIXE is a non-destructive analysing technique (Kristensson, et al., 2019) (Prosper, 2017).

To collect 24 hours samples of PM_{10} for PIXE analysis, a Gent stacked filter unit (SFU) sampler was used. The Gent sampler contains an impactor plate at the inlet, for which particles with a larger diameter than 10 micrometers impact and collects. The impactor plate was covered with a thin layer of grease to reduce the bounce off effect. The stacked filter unit contained a polycarbonate track-etched filter by Sartorius with 0,4 µm pore size, collecting the PM_{10} fraction of particles. The Gent SFU were connected with tubes and Swagelok connections to a flow valve, in order to control the flow rate through the sampling unit. The flow valve was connected to a pump with tubes and Swagelok connections, pumping the air through the system. Figure A1 shows a schematic overview of the setup. The filters in the SFU were changed manually after 24 hours of sampling, achieving daily measurements.

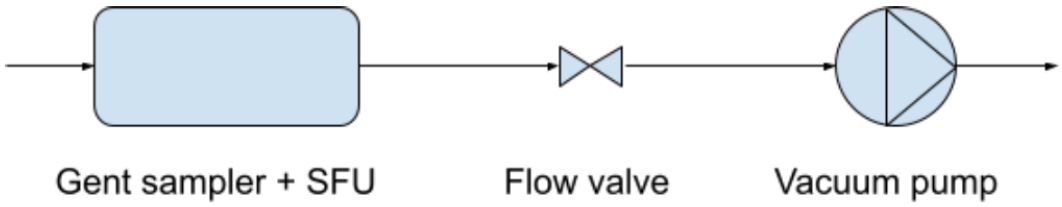

Figure A1: Schematic overview of the setup for the PIXE measurement, with a Gent sampler and SFU, flow valve and a vacuum pump.

The flow of 16.7 l/min was used to separate particles larger than 10 µm. In an impactor the aerosols flow through a nozzle towards an impaction plate by which the direction of the flow changes direction by 90 degrees. This causes larger particles, with a higher inertia, to collide with the impaction plate while particles with a smaller inertia follow the streamlines change in direction. The collection efficiency is the fraction of particles collected on the impaction plate and is a function of particle size. Ideally the collection efficiency curve has a sharp cut-off size (d_{50}), where all particles larger than the cut-off size is collected on the impaction plate and all particles smaller than the cut-off size passes through (Hinds, 1999).

When the collection efficiency curve is not ideal, some particles larger than the cut-off size will get through and some smaller particles will be collected on the impaction plate. Collection efficiency depends on Stokes number (Stk), which is the ratio between stopping distance (τ) and nozzle velocity (U) and nozzle radius ($D_j/2$), see Equation A1. The square root of Stokes number is proportional to particle size and the cut-off diameter d_{p50} can be calculated from Equation A1, where d_p is particle diameter, ρ_p is particle density, η is the viscosity of air and C_c is the Cunningham slip correction factor. Stk_{50} is when 50% collection efficiency occurs and characterizes where the ideal cut-off curve fits the actual cut-off curve the best. At Stk_{50} the mass

of larger particles that are not collected equals the mass of smaller particles that are collected that ideally should have passed through. The ideal and actual collection curve are shown in Figure A2 (Hinds, 1999).

Equation A1

$$Stk = \frac{\tau U}{D_j/2} = \frac{\rho_p d_p^2 U C_c}{9\eta D_j}$$

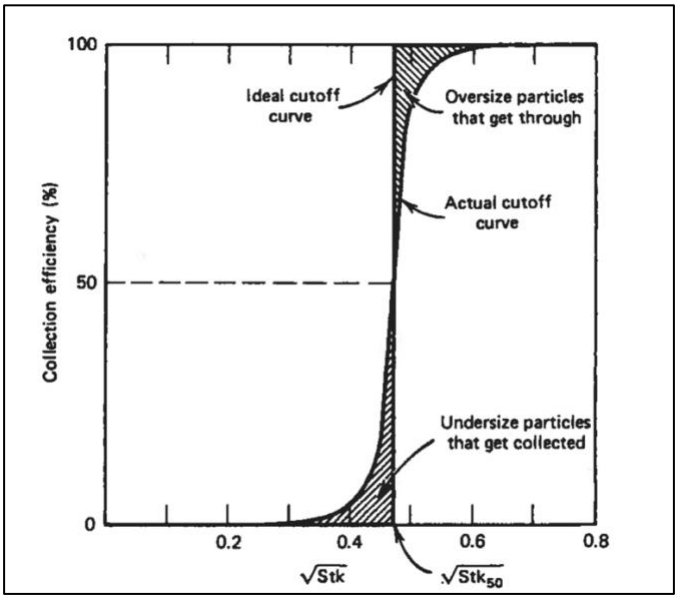

Figure A2: Ideal and actual cut-off curve with collection efficiency on the y-axis and the square root of Stokes number on the x-axis (Hinds, 1999).

Appendix B – Metals detected below 85% of the samples

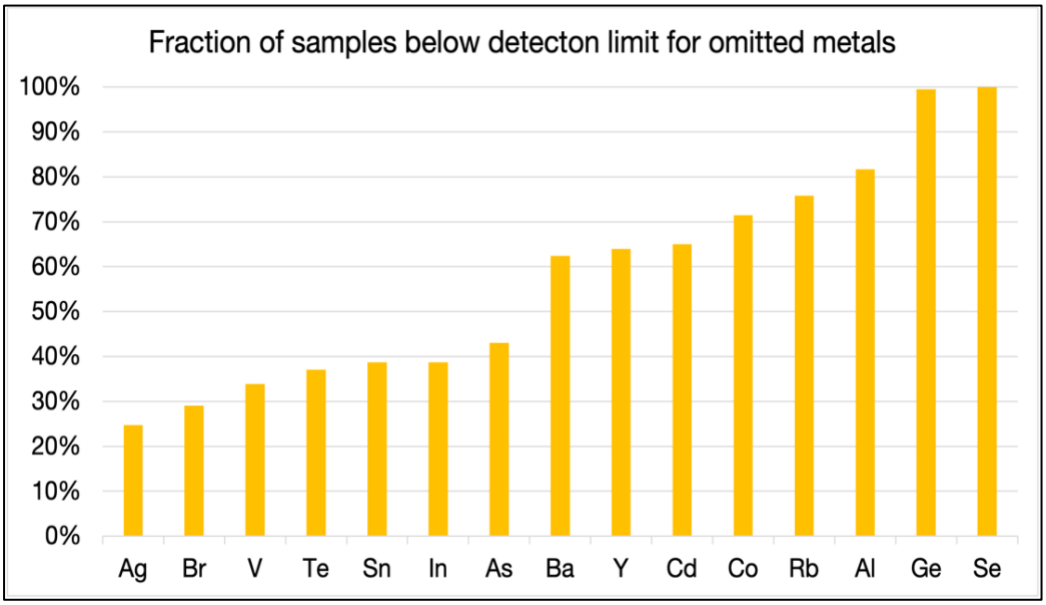

Figure B1: The 15 out of the 33 elements that the Xact is capable of measuring that were detected less than 85% of the samples. The fraction of samples below the detection limit is visible.

Appendix C – Diurnal concentrations

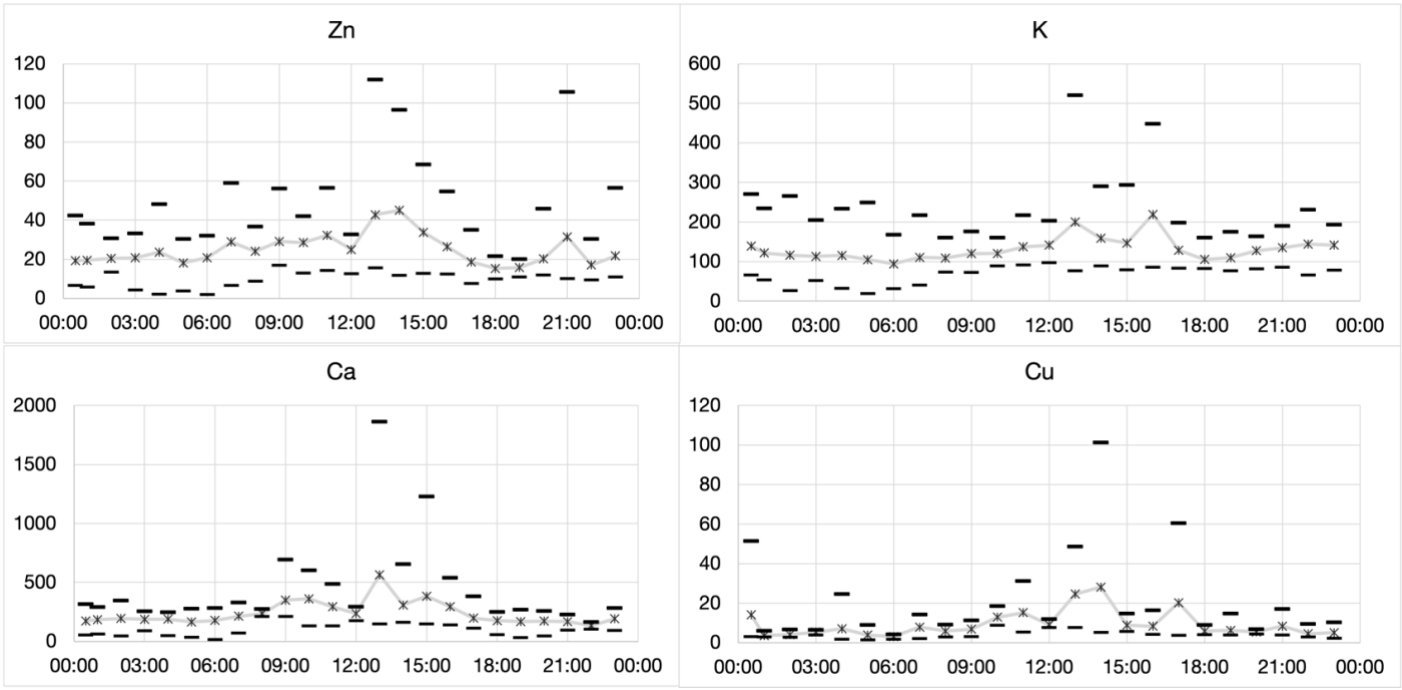

Figure C1: Diurnal concentration for Zn, K, Ca and Cu.

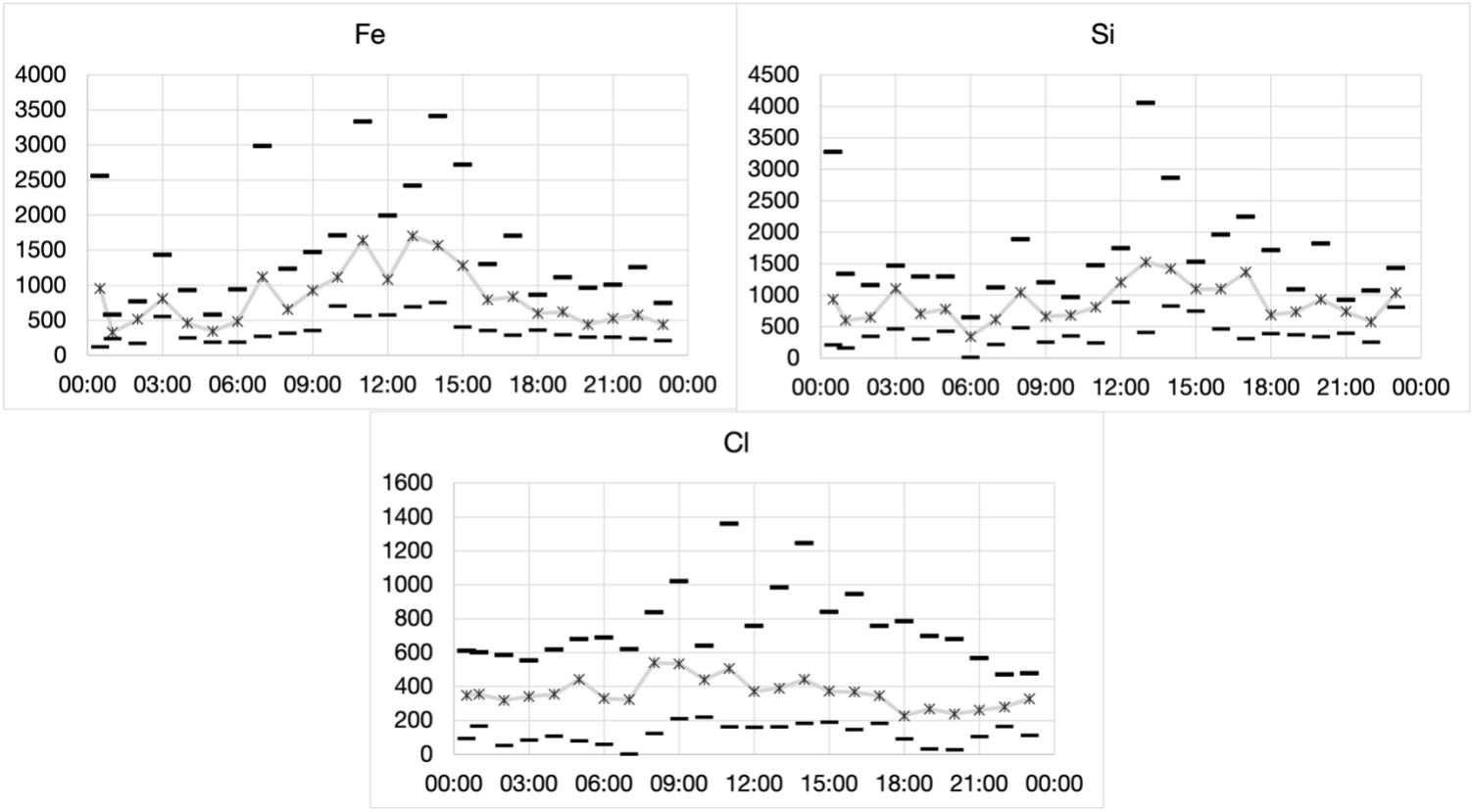

Figure C2: Diurnal concertation for Fe, Si and Cl.

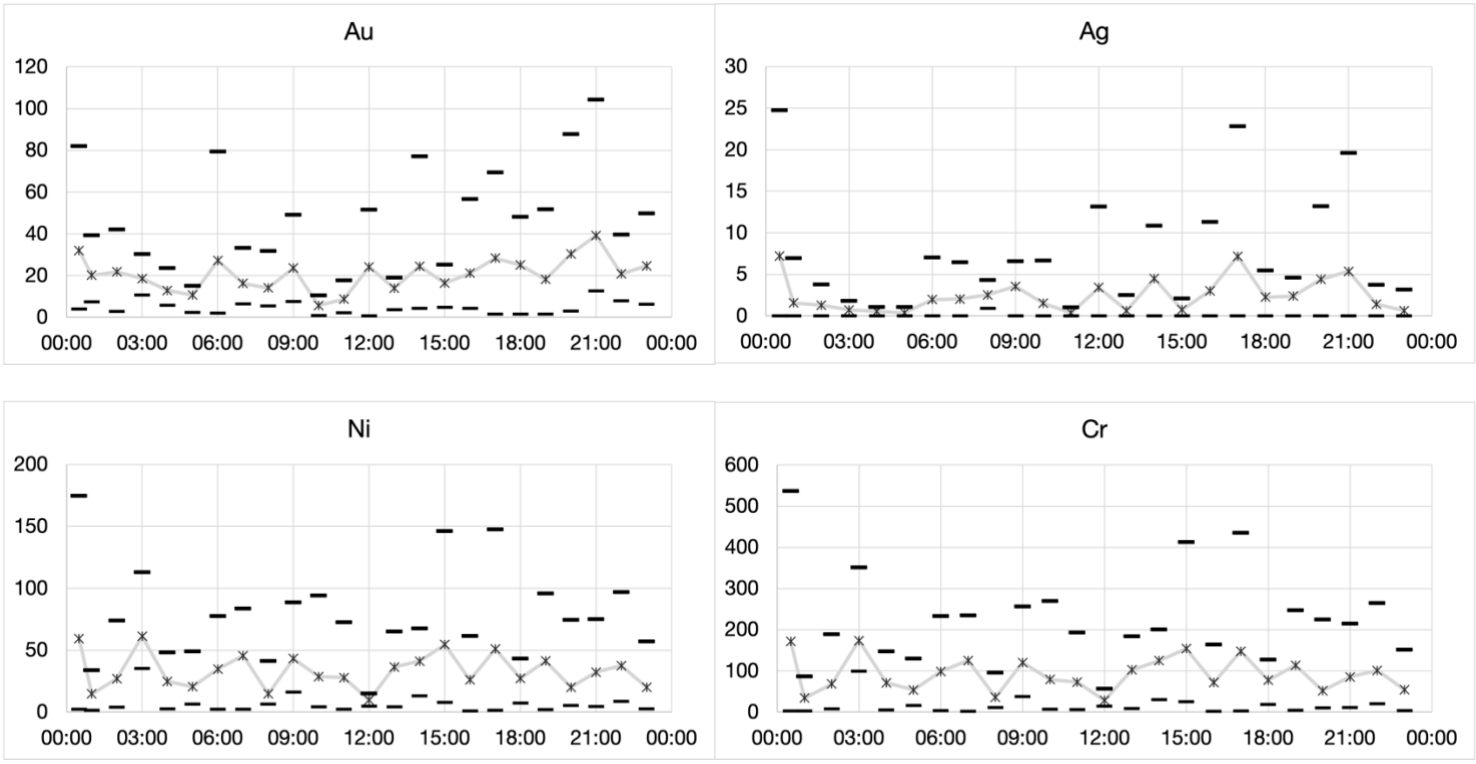

Figure C3: diurnal concentration for Au, Ag, Ni and Cr.

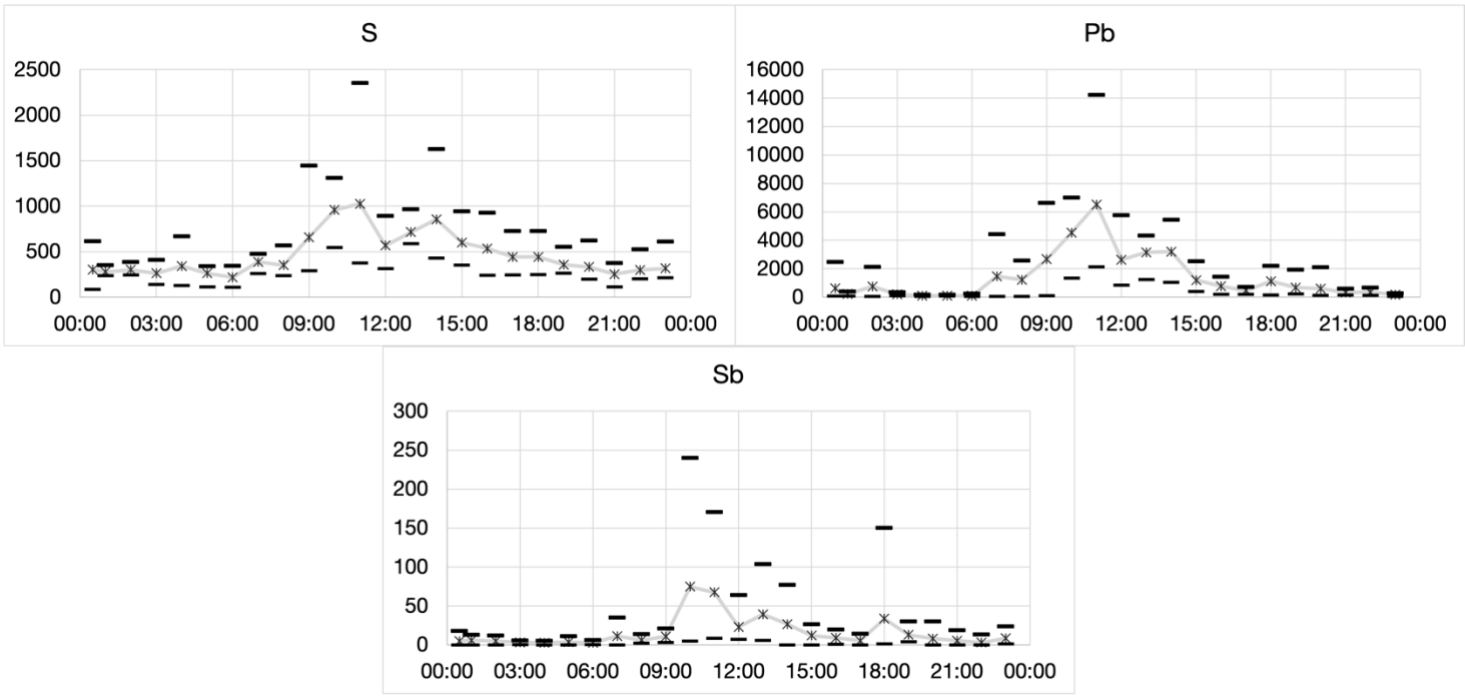

Figure C4: diurnal concentration for S, Pb and Sb.

Appendix D – Detailed activity-concentration graphs

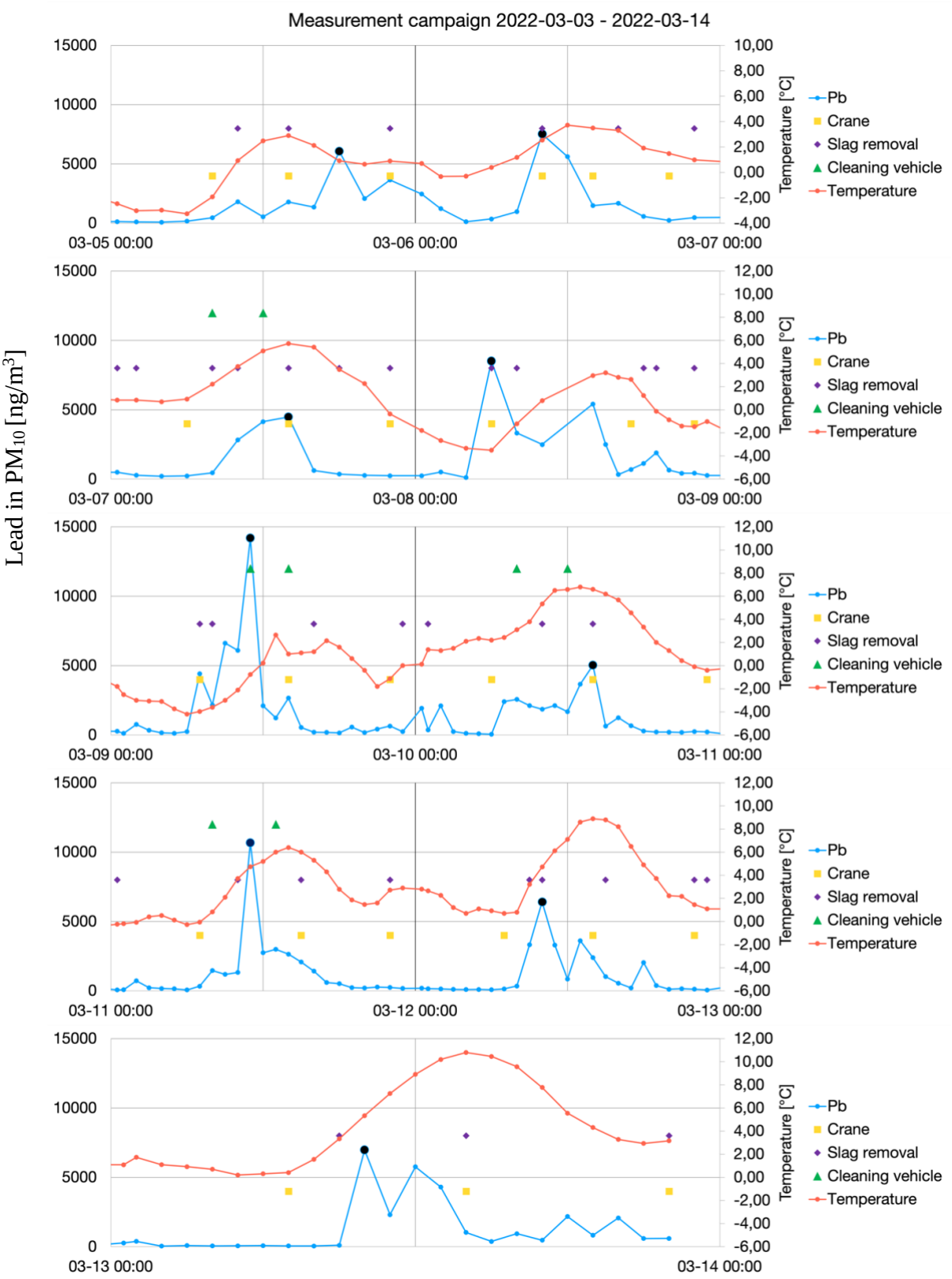

Figure D1: Detailed activity – concentration graphs for the measurement period. The daily maximum concentration is highlighted with black circles.